Regulatory T-cells in multiple sclerosis are activated by Epstein-Barr Virus and produce IL-10 in the central nervous system

N. Pulvirenti[1], C. Righetti[1], F. Clemente[1], B. Serafini[2], A. Pietroboni[3], E. Galeota[1], B. Rosicarelli[2], C. Cordiglieri[1], C. Iannone[8,9], M. de Riz[3], C. Vasco[1], A. Espadas de Arias[4], T. De Feo[4], L. Valenti[5,6], D. Prati[6], S. Abrignani[1,7], M. Gerosa[7,8], R. Caporali[8,9], D. Galimberti[3,9], E. Scarpini[3,9], J. Geginat[1,7]

1 Fondazione Istituto Nazionale di Genetica Molecolare, Milan, Italy

2 Department of Neuroscience, Istituto Superiore di Sanità, Rome, Italy

3 Neurology-Neurodegenerative Diseases Unit, Fondazione IRCCS Ca' Granda Ospedale Maggiore Policlinico, Milan, Italy

4 Laboratorio di Immunologia dei Trapianti - S.C. Trapianti Lombardia-NITp - Fond. IRCCS Cà Granda Ospedale Maggiore Policlinico, Milan, Italy

5 Department of Pathophysiology and Transplantation, Università degli Studi di Milano, Italy

6 Transfusion Medicine, Fondazione IRCCS Ca' Granda Ospedale Maggiore Policlinico, Milano, Italy

7 Department of Clinical Sciences and Community Health, Università degli Studi di Milano, Italy

8 Centro Specialistico Ortopedico Traumatologico Gaetano Pini - CTO, Milan, Italy

9 Department of Biomedical, Surgical and Dental Sciences, Università degli Studi di Milano, Italy

Abstract

Regulatory T-cells (Tregs) maintain immune homeostasis, but antigens activating adaptive Tregs in human pathologies are ill-defined. EOMES$^+$type-1 regulatory (EOMES$^+$Tr1-like) T-cells had a dysregulated homeostasis in multiple sclerosis (MS), which was related to their activation in the central nervous system (CNS). EOMES$^+$Tr1-like cells were strongly enriched in patient's cerebrospinal fluid (CSF) and were the main IL-10-producing T-cells in the CSF. IL-10$^+$EOMES$^+$Tr1-like were present in MS brain lesions, and some were found close to Epstein-Barr Virus (EBV)-infected B-cells. EOMES$^+$Tr1-like cells and FOXP3$^+$Tregs produced IL-10 with EBV-derived antigens, but not with major myelin antigens. EOMES$^+$Tr1-like cells responded selectively to the latency-associated antigen EBNA1, whereas FOXP3$^+$Tregs responded also to lytic antigens. EBNA1-specific EOMES$^+$Tr1-like cells were associated with anti-EBNA1 IgG, disappeared upon therapeutic B-cell depletion and were relatively abundant in patients with the HLA-DRB1*15 risk haplotype. The aberrant anti-viral specificities of Tregs in MS could undermine their protective functions and anti-EBV immune surveillance.

Introduction

Natural regulatory T-cells (Tregs) are generated in the thymus, express the transcription factor FOXP3 and are required to prevent autoimmunity[1,2]. A reduced number or functionality of FOXP3$^+$Tregs to control the activation of autoreactive T-cells is therefore thought to play a crucial role in many autoimmune diseases[3]. FOXP3$^+$Tregs can however also be generated in the periphery in response to foreign antigens, which may be derived from pathogens[4]. Some regulatory T-cells lack FOXP3 expression but produce high levels of the anti-inflammatory cytokine IL-10[5]. These IL-10 producing "type 1 regulatory T(Tr1)-cells" are adaptive Tregs, which are generated in the periphery in response to self- or foreign antigens[6,7], and require thus TCR stimulation by specific antigens for their functions[8]. Tr1-cells are highly heterogeneous[9]. They may produce IL-10 alone or together with IFN-γ[10-13] and inhibit excessive immune responses and immunopathology[13]. During persistent viral infections, IL-10 and IFN-γ co-producing Tr1-like cells are generated upon chronic antigenic stimulation and inhibit collateral tissue damage, but also viral clearance[7,14]. In an increasing number of pathologies, including chronic viral infections, IL-10 and IFN-γ co-producing Tr1-like cells were reported to express the transcription factor EOMESODERMIN (EOMES) and the cytotoxic molecule Granzyme-K (GzmK)[6,15-19]. Like FOXP3$^+$Tregs, EOMES$^+$Tr1-like cells can suppress CD8$^+$T-cell responses[17], the key effector cells that control viral infections. Not all EOMES-expressing CD4$^+$T-cells are however Tr1-like cells, since those expressing CCR6 or GzmB have pro-inflammatory properties[20-22]. However, pro-inflammatory EOMES$^+$GzmK$^+$T-cells may possess suppressive capabilities[22], and differentiate to anti-inflammatory EOMES$^+$Tr1-like cells upon chronic antigenic activation in a negative feedback loop to inhibit immunopathology[13,18,23].

Multiple sclerosis (MS) is the most common chronic inflammatory demyelinating disease of the central nervous system (CNS) with a prevalent relapsing-remitting (RR-MS) onset that can evolve into a progressive course (P-MS). The aetiology is still unclear, but both genetic and environmental factors contribute critically to the overall disease risk[24]. The strongest genetic risk factor is the human leukocyte antigen (HLA) class II allele HLA-DRB1*15:01 which encodes an MHC class 2 molecule that could present critical self-peptides to activate autoreactive CD4$^+$T-cells[25]. Among environmental factors, infection with the almost ubiquitous herpesvirus Epstein-Barr Virus (EBV) is a necessary, although not sufficient, condition for initiating

inflammatory brain damage leading to MS[26]. EBV-associated infectious mononucleosis and anti-Epstein Barr Virus nuclear antigen (EBNA)1 IgG levels interact with HLA-DRB1*15:01 to increase the risk of MS. However, the mechanism by which EBV promotes MS is debated and a focus of intense reasearch[14,27-29]. Accumulating evidence indicates an altered immune response to EBV in MS, and it was proposed that anti-EBV immune surveillance may be inefficient in MS[30].

Regulatory T-cells are thought to be reduced and/or defective in MS, since they fail to prevent CNS damage. MS-like disease symptoms were however not reported in FOXP3-deficient mice or patients[2], and reduced FOXP3$^+$Treg numbers are not consistently associated with MS[31]. FOXP3$^+$Tregs proliferate however less upon TCR stimulation in MS[32], produced higher amounts of IFN-γ but lower amounts of IL-10, and may be functionally impaired[33,34]. Tr1-like cells producing IL-10 and IFN-γ were shown to play a protective role in experimental autoimmune encephalomyelitis (EAE), a widely used animal model of autoimmunity-driven CNS inflammation[35]. Moreover, the *in vitro* generation of IL-10 producing CD4$^+$T-cells was defective in MS[36], suggesting that the differentiation of potentially protective Tr1-cells may be impaired. However, if EOMES$^+$Tr1-like cells are involved in MS or anti-EBV immune control is unknown[18]. Notably, EOMES expression in CD4$^+$T-cells promoted CNS inflammation in EAE[37], suggesting that pro-inflammatory EOMES$^+$T-cells could promote CNS damage. Moreover, cytotoxic CD4$^+$EOMES$^+$GzmB$^+$T lymphocytes (CTL) were proposed to play a pathogenic role in MS[38,39]. Here, we investigated the features of EOMES$^+$Tr1-cells in MS. We found that they were activated *in vivo,* produced high amounts of IL-10 and accumulated in the CNS. However, they were specific for EBV-derived antigens, suggesting that they promote EBV immune escape but are inefficient to prevent CNS damage.

Materials and Methods

Human samples

Patient samples were collected at the MS Centre of the *Fondazione Ca' Granda, IRCCS Ospedale Policlinico*, Milan ("Policlinico"), upon written informed consent, after Institutional Ethical Committee approval (parere 708_2020). Patients were diagnosed according to the revised McDonald criteria[40]. We collected 6-8 ml of peripheral blood samples, by venous puncture, from 13 treatment-naïve patients affected by RR-MS (1-3d after an attack), 4 untreated P-MS patients, 22 Natalizumab-treated RR-MS patients and 17 Ocrelizumab-treated MS patients (containing both RR and P-MS). For the latter, blood was collected before the therapy session. 3-7 ml of CSF samples were obtained by lumbar puncture from 7 untreated patients at diagnosis. In 5 of these patients also paired blood samples were obtained. All patients whose CSF was analysed, were diagnosed as RR-MS and had not received any previous treatment. Demographic and clinical characteristics of MS patients and healthy donors (HD) enrolled in the study are shown in Table 1. As controls, 78 age- and sex-matched healthy donors were enrolled at the Policlinico upon informed consent.

Table 1 Characteristics of PwMS and HD

	Healthy Donors	Treatment naive RR-MS	NTZ-treated RR-MS	Untreated P-MS	OCR-treated MS	Untreated MS (OCR Ctr)
Number of subjects	78	13	22	4 (3PP, 1SP)	17 (8 PP, 3 SP, 6 RR)	13 (3 PP, 10 RR)
Female/male (ratio)	47/31 (1.5)	7/6 (1.2)	14/10 (1.4)	0/4 (0)	7/10 (0.7)	5/8 (0.6)
Age, median (range)	34 (20-61)	34 (20-51)	35 (20-62)	48 (28-69)	47 (25-69)	44 (20-69)
EDSS T0, median (range)	n.a.	1.0 (0.0-2.0)	2.0 (1.0-5.5)	2.8 (2.5-4.5)	3.5 (0.0-6.5)	1.0 (0.0-4.5)
EDSS T1 (2023), median (range)	n.a.	1.0 (0.0-2.5)	2.0 (1.0-6.0)	3.0 (2.5-4.5)	3.5 (0.0-7.0)	1.5 (0.0-4.5)

EDSS: Expanded Disability Status Scale; MS: Multiple Sclerosis; NTZ: Natalizumab; OCR: Ocrelizumab; P: Progressive; PP: Primary Progressive; RR: Relapsing-Remitting; SP: Secondary Progressive

In addition, we collected blood from 17 SLE patients with and without CNS involvement.

Table 2 Characteristics of SLE patients

	SLE w/o CNS	SLE CNS
Number of subjects	11	6
Female/male	8/3	6/0
Age, median (range)	41 (21-57)	40 (25-60)
SLEDAI, median (range)	2 (0-8)	4 (0-12)

Cell isolation

Peripheral blood mononuclear cells (PBMCs) were isolated from heparinized peripheral blood by Ficoll-Hypaque gradient within 24h from blood withdrawal. Cells from CSF were collected by centrifugation and analysed immediately. Plasma was collected and decomplemented or stored at -80°C until use.

Cell stimulation

PBMC were incubated for 4h at 37°C in a 5% CO2 humidified atmosphere at a density of 2,5 x 10^6 cell/mL in RPMI complete medium (2 mM glutamine, 1 mM sodium pyruvate, 1% non-essential amino acids, 1% penicillin/streptomycin) supplemented with 10% FCS in presence or absence of PMA (50 ng/mL) and Ionomycin (500 ng/mL). After 2h, Monensin (0.6 µl/ml,) was added and stimulated cells were stained for superficial and intracellular markers (listed in sTable 4). For antigen -specific stimulations cells were stimulated for 5 hours with peptide pools (EBV: Pool from 15 EBV proteins, or overlapping peptide pools from EBNA1, BZLF1, BMRF1; JCV: VP1 plus VP2; Myelin: MOG, MBP, PLP, Miltenyi) in medium without FCS that contained 5% autologous plasma. Incubation without peptides was analysed as negative control, and with 100 ng/ml of the super-antigen SEB as positive control.

Flow Cytometry

Cells were stained at the surface and intracellularly with fluorochrome-conjugated monoclonal antibodies and live/dead exclusion dye. The different panels of antibodies (Ab) are represented in sTable 4. For surface staining, PBMCs were incubated for 20 min at 37°C, with the appropriate antibodies, including a live/dead (L/D) dye, diluted in Brilliant Staining Buffer (BD). After incubation, unbound antibodies were removed by washing the cells. To

stain for intracellular molecules samples were fixed with the Fixation/Permeabilization working solution (eBioscience). For cytokine detection following PMA plus Ionomycin stimulation cells were fixed with 2% PFA. Fixed cells were permeabilized for 20 min at RT (eBioscience Permeabilization Buffer), washed and resuspended with the antibody cocktail diluted in permeabilization buffer. Cells were incubated at 4°C for 60 minutes. Finally, samples were washed, resuspended in PBS, acquired on a BD FACSymphony and analysed with the BD FACSDiva Software. Antigen-specific $CD4^+$ and $CD8^+$T-cells were gated as $CD69^+$IFN-γ^+ unless otherwise indicated, Tregs were gated as 4-1BB^+CD69^{+}[41]. Antigen-stimulated $CD4^+$T-cell subsets cells were in some cases also analysed for IL-10 production (sFigure 4A-C). Notably, the markers used to identify T-cell subsets (CD4, CD8, IL-7R, CCR6, FOXP3, GzmK, GzmB[42]) were stably expressed in the analysed time window (sFigure 4D).

Anti-EBNA1 ELISA

ELISA to measure the levels of anti-EBNA1 IgG were performed using serum diluted 1:5 with a kit (Serion Diagnostics) following the manufacturer's instructions.

Tissue samples and immunostainings

Sections from 5 well-characterized post-mortem brain tissue blocks from 4 donors with progressive MS, provided by the UK Multiple Sclerosis Tissue Bank at Imperial College London (https://www.imperial.ac.uk/medicine/multiple-sclerosis-and-parkinsons-tissue-bank/) were analysed. The use of human tissue for research purposes was approved by the Ethics Committee of Istituto Superiore di Sanità (2023_0059846). Sections from a human thymus and from an axillary lymph node were used as internal controls of the IHC procedures. Tissue sections used in this study contained substantial immune infiltrates with CD4+ and CD8+ T cells in the white matter (WM) and meninges. Triple immunostainings in bright field were performed with mouse anti-EOMES, rat anti-IL-10 and rabbit anti-CD4 purified monoclonal antibodies (see supplementary Methods). Negative control stainings were performed in consecutive sections using rat and mouse Ig isotype controls (ThermoFisher, sFigure 7).

In serial sections immunostainigs for CD8, CD20 and EBER[43] and double stainings with rabbit polyclonal anti-CD8 (Thermo Fisher Scientific) and anti-EOMES were also performed. Stained

sections were analysed and images acquired with an Axioscope microscope (Carl Zeiss, Jena, Germany) equipped with AxioCam MRc5 camera and Axiovision SE 64 software. Cell counts were performed manually in the immune infiltrates containing $CD4^+$ cells on the entire sections, both the WM and meninges, with a morphometric grid within the ocular lens, at 20x magnification. Data are expressed as mean $\pm$SD values of the percentages of triple positive $EOMES^+IL10^+CD4^+$ cells in the total $CD4^+$T-cell population.

Statistical analysis

Data were analysed with FlowJo software (Tree Star Inc, v. 10.8), while the statistical analyses were performed with Prism10 software (GraphPad). Student t-test were performed to compare two groups, a paired t-test for values derived from the same individuals, and an unpaired t-test to compare two different cohorts. One-way ANOVA was used to compare a single parameter in multiple groups, two-way ANOVA to compare multiple values in multiple groups. P-values <0.05 (*), <0.01 (**), < 0.005 (***) were regarded as statistically significant. Where indicated, borderline p-values (0.05-0.1) were reported in the panels.

scRNAseq data

Processed single-cell RNA sequencing (scRNA-seq) gene expression data were obtained from the Gene Expression Omnibus (GEO) database under the accession number GSE232343[44]. The data were subsequently analyzed using the Seurat package (v.5.0.1) in R. The scRNA-seq dataset contained clusters defined in the original study. We utilized Seurat's FindAllMarkers function with default parameters to obtain Differentially Expressed Genes (DEGs) for each cluster. Clusters were labelled using the DEGs and additional information of known $CD4^+$T-cell subset markers. To identify DEGs between conditions within the same $CD4^+$T-cell subpopulation, we employed a pseudobulk approach. This method aggregates single-cell counts within each condition/patient to create bulk-like profiles, thereby improving the robustness of the differential expression analysis. Gene set enrichment analysis (GSEA) was performed using the fgsea() function from the fgsea package (v1.20.0). The reference Tr1 associated gene set for the analysis was obtained from our previous studies[17,45].

Results

The homeostasis of EOMES$^+$Tr1-like cells is dysregulated in MS.

T-cell subsets in recently diagnosed, treatment-naive PwMS and age and sex-matched HD (Table 1) were monitored in peripheral blood by multidimensional flow cytometry. Bioinformatic analysis of T-cells from peripheral blood (PB), based on unsupervised clustering and dimensionality reduction algorithm, identified 27 T-cell clusters (Figure 1A, sFigure 1A/B), including 12 CD4$^+$ clusters. Cluster 11 displayed the phenotype of EOMES$^+$Tr1-like cells (i.e. CD4$^+$EOMES$^+$GzmK$^+$CCR5$^+$PD1$^+$CD27$^+$CCR6$^-$[18,19,46], sFigure 1C), and co-clustered with CD4$^+$EOMES$^+$T-cells that expressed CCR6 (Cluster (Cl) 10, sFigure 1C). In the Uniform Manifold Approximation and Projection (UMAP) maps (Figure 1A) these two GzmK$^+$CD4$^+$T-cell clusters were positioned in the centre of Th1-cells (Cl 5), Th1/17-cells (Cl 6,8) and CD4$^+$GZMB$^+$CTL[45] (Cl 12), consistent with an intermediate differentiation stage[22,45]. Surprisingly, we detected no major differences in the compositions of the T-cell compartments in the blood of PwMS and HD (Figure 1A), but we observed some minor variations among the cytotoxic CD4$^+$T-cell clusters (Cl 4, 10-12). We therefore analysed EOMES$^+$CD4$^+$T-cell subsets more in detail exploiting an established gating strategy to distinguish EOMES-expressing GzmK$^+$ and GzmB$^+$("CD4$^+$CTL") subsets from FOXP3$^+$Tregs and the majority of helper T-cells ("Th", sFigure 1D, E)[19,42]. GzmK$^+$T-cells were further subdivided according to the expression of CCR6 into pro-inflammatory CCR6$^+$ and Tr1-containing CCR6$^-$ subsets[21,46] (sFigure 1C-F). Also with this strategy we detected no significant alterations among CD4$^+$T-cells in RR- or in P-PwMS as compared to HD (sFigure 1G). However, focussing the analysis on GzmK$^+$CCR6$^-$IL-7R^{lo}T-cells[6,19], which contained by far the highest frequencies of IL-10-producing T-cells (sFigure 1F)[22], unveiled a significant decrease of these Tr1-like effector cells in both P- and RR-MS patients (Figure 1B). In contrast, pro-inflammatory CCR6$^+$GzmK$^+$ cells were increased in RR-MS, whereas CD4$^+$CTL were increased in P-MS (sFigure 1G). However, these increases did not reach statistical significance. Notably, in RR-PwMS treated with Natalizumab Tr1-like effector cells were not significantly reduced as compared to HD. Since Natalizumab blocks the adhesion receptor VLA-4 and consequently lymphocyte homing to the CNS, this finding suggested that the reduced frequencies of Tr1-like cells in untreated PwMS may be related to CNS homing[47]. Consistently, major fractions of EOMES$^+$Tr1-like cells, but also of CCR6$^+$GzmK$^+$ cells and of CD4$^+$CTL, expressed VLA-4 (Figure 1C), indicating that they possess a high CNS

homing potential. Conversely, only minor fractions of FOXP3$^+$Tregs and Th-cells were VLA-4$^+$. This pattern was observed in both HD and PwMS.

We finally investigated *in vivo* proliferation rates according to Ki67 expression. Th-cells and CCR6$^+$GzmK$^+$ cells were largely quiescent, whereas minor fractions of CTL, Tregs and EOMES$^+$Tr1-like cells expressed Ki67, indicating recent *in vivo* proliferation (sFigure 1H). Importantly, we observed a significant increase of Ki67 expression in IL-7R^{lo}EOMES$^+$Tr1-like effector cells in PwMS compared to HD (Figure 1D). Proliferation of FOXP3$^+$Tregs[32] and CD4$^+$CTL was in contrast reduced (sFigure 1H). Moreover, EOMES$^+$Tr1-like cells had significantly reduced Ki67 expression in Natalizumab-treated as compared to treatment-naive RR-PwMS (Figure 1D), suggesting that CNS homing may lead to their activation. Notably, a similar tendency was observed for FOXP3$^+$Tregs (sFigure 1H).

Overall, these findings indicate that EOMES$^+$Tr1-like-cell homeostasis is dysregulated in MS and suggest that this alteration is related to CNS homing.

EOMES$^+$Tr1-like cells are strongly enriched in the cerebrospinal fluid of PwMS.

In order to investigate if EOMES$^+$Tr1-like cells could be recruited to the CNS, we interrogated a single cell RNA sequencing dataset of antigen-experienced CD4$^+$T-cells from paired CSF and blood samples of untreated PwMS and control donors with idiopathic intracranial hypertension[44]. To avoid any bias, we adopted the reported bioinformatic strategy and regenerated the same UMAP (Figure 2A). Considering all differentially expressed genes (DEGs) in the 13 clusters (sTable 1), as well as selected subset-associated marker genes (sFigure 2A,B), we confirmed that cluster 13 corresponded to FOXP3$^+$Tregs, and annotated in addition clusters containing cTFH (Cl 1), cells with an IFN signature (Cl 3), Th17-cells (Cl 4), GzmK^{lo}Th1-like cells (Cl 8), Th2-cells (Cl 10) and CD4$^+$CTL (Cl12, Figure 2A). Since cells in cluster 2 expressed stemness-associated genes (sFigure 2A) they were named T_{CM}, whereas the remaining three Clusters (Cl 5, 6 and 9) lacked a clear gene signature and were named T_{EM}A, B and C, respectively. Importantly, cluster 7 displayed the gene signature of EOMES$^+$Tr1-like cells[17,19,45] (Figure 2B), as evidenced by a highly significant Gene Set Enrichment Analysis (GSEA). Indeed, several key EOMES$^+$Tr1-like signature genes, namely EOMES[19], CHI3L2[17], CCR5 and PDCD1 (PD1)[46] and CCL4 were rather selectively expressed in this cluster (Figure 2C). Moreover, they expressed the highest levels of GzmK, low levels of IL-7R and lacked CCR6 (Figure 2D, sFigure 2A)[19]. Other putative Tr1-associated genes like LAG3, ITGA2 (CD49b)[9],

CTLA-4 and HVACR2 (TIM3) were in contrast not specifically associated with this cluster (sFigure 2C). Also cells in Cluster 11 expressed GzmK and EOMES, but they expressed in addition CCR6 and high levels of IL-7R (Figure 2D, sFigure 2D), suggesting that they corresponded to the CCR6$^+$GzmK$^+$ subset. This CCR6$^+$GzmK$^+$ cluster was separated in the UMAP from EOMES$^+$Tr1-like cells by the GzmK^{lo}Th1-like cluster (Cl 8, Figure 2A), suggesting that they had largely diverse gene expression patterns. Indeed, cells in the CCR6$^+$GzmK$^+$ cluster lacked EOMES$^+$Tr1-like signature genes (Figure 2C, E) and over-expressed instead CD40L and genes characteristic for pro-inflammatory Th1/17-cells, including RORC, IL-23R, IL-12Rβ2 and IL-18R (sTable 2, Figure 2E, sFigure 2D). Interestingly, also Tregs expressed IL-12Rβ2 in PwMS, consistent with a Th1-like polarization[34]. Notably, the EOMES$^+$Tr1-like cluster in the CSF of PwMS expressed the highest levels of EOMES$^+$Tr1-like signature genes (Figure 2E). They had also an altered expression of genes regulating cholesterol metabolism, but this was a general feature of CSF-infiltrating CD4$^+$T-cells (sTable 3, sFigure 2E)[48].

Importantly, only the EOMES$^+$Tr1-like cluster was strongly, selectively and significantly increased in the CSF as compared to the blood (Figure 2F, sFigure 2F). Conversely, the CCR6$^+$GzmK$^+$ cluster was slightly reduced, and CD4$^+$CTL (Cl 12), as well as the T_{EM}C cluster (Cl 9) were largely restricted to the blood. This was observed both in PwMS and in control donors. To corroborate the enrichment of EOMES$^+$Tr1-like cells in the CSF, we analysed CD4$^+$T-cell subsets from the blood and the CSF in an independent cohort of treatment-naive RR-PwMS (Table 1) by flow cytometry. EOMES$^+$Tr1-like cells were confirmed to be highly enriched in the CSF (Figure 2G). Conversely, the frequencies of Th-cells, CCR6$^+$GzmK$^+$T-cells, FOXP3$^+$Tregs and CD4$^+$CTL were not significantly different.

CXCR3 gene expression was increased in EOMES$^+$Tr1-like in the CSF (Figure 2E, sTable 3), and is involved in CNS homing[27,44]. Notably, EOMES$^+$Tr1-like and CCR6$^+$GzmK$^+$ cells contained the highest frequencies of CXCR3$^+$ cells in peripheral blood of RR-PwMS (Figure 2H). Furthermore, the percentage of CXCR3-expressing cells was strongly and significantly increased on all CD4$^+$T-cells in the CSF, and virtually all EOMES$^+$Tr1-like cells in the CSF were CXCR3$^+$. Finally, also the large majority of Ki67$^+$EOMES$^+$Tr1-like cells expressed CXCR3, while CXCR3 expression on most other proliferating T-cell subsets was significantly lower (sFigure 2G).

Collectively, these results show that EOMES$^+$Tr1-like cells can be identified in an unbiased manner according to their unique gene expression profile in PwMS, possess high CNS homing potential and are strongly and selectively enriched in the CSF.

EOMES$^+$Tr1-like cells are the major IL-10 producing T-cell subset in the CSF of PwMS.

A few IL-10$^+$ cells could be detected by single cell RNA sequencing[44], and, intriguingly, they belonged mostly to the EOMES$^+$Tr1-like cluster. These IL-10$^+$Tr1-like cells co-expressed virtually all GzmK, but not FOXP3 (Figure 3A) and they were predominantly IL-7R^{lo} (sFigure 3A), suggesting that they represented *in vivo* activated Tr1-like effector cells. Consistently, some IL-7R$^-$Tr1-like cells expressed also IFN-γ, but not IL-2. In contrast to IL-10$^+$T-cells, IFN-γ$^+$ and IL-2$^+$T-cells were present in several different clusters, and most of them co-expressed IL-7R (sFigure 3A).

We next analysed cytokine producing capacities of CD4$^+$T-cells in the CSF and in peripheral blood of PwMS following brief polyclonal stimulation *ex vivo*. Unsupervised clustering identified 10 T-cell clusters, including a single IL-10$^+$ cluster (Cl 9) that co-expressed EOMES, GzmK and IFN-γ and corresponded thus to EOMES$^+$Tr1-like cells (sFigure 3B). The nine IL-10-negative clusters separated according to effector cytokine production (sFigure 3B). In the CSF there was a strong enrichment for effector clusters (Figure 3B, Cl 2-4 and 7-9). Cells in the IL-10-negative effector cluster 8 contained pro-inflammatory EOMES$^+$GzmK$^+$cells that expressed CD40L, IFN-γ and GM-CSF[49]. In the blood most CD4$^+$T-cells expressed instead exclusively CD40L (Figure 3B, Cl 1). We next investigated possible differentiation pathways of the identified T-cell clusters by DiffusionMap analysis (Figure 3C, sFigure 3C). Dimension 1 separated clusters according to effector cytokines into a non-polarized and an effector group. Dimension 2 separated clusters furthermore according to CD40L expression into helper and regulatory/effector cells. IL-10$^+$Tr1-like cells were positioned on top of the pro-inflammatory GzmK$^+$ cluster, consistent with a precursor-effector relationship[18,22].

Notably, EOMES$^+$Tr1-like cells contained consistently the highest percentages of IL-10$^+$T-cells of all CD4$^+$T-cell subsets (Figure 3D). *Ex vivo* IL-10 production by CD4$^+$T-cell subsets was not significantly reduced in the blood of PwMS, but it was increased in EOMES$^+$Tr1-like cells in the CSF. Of note, EOMES$^+$Tr1-like cells produced high amounts of IL-10 in the CSF of both RR- and P-MS patients (sFigure 3D). Also IFN-γ production by EOMES$^+$Tr1-like- and Th-cells was increased in the CSF (Figure 3D, sFigure 3D), and a not-significant tendency was evident for FOXP3$^+$Tregs[34].

Although only a very small fraction of Th-cells produced IL-10, they were the large majority of CD4$^+$T-cells and constituted consequently also the majority of IL-10 producing T-cells in the

blood (Figure 3E). Conversely, in the CSF of PwMS the major IL-10 producing T-cell subset were EOMES$^+$Tr1-like cells. In addition, also the contribution of Tregs to the pool of IL-10-producing CD4$^+$T-cells was increased in the CSF.

In conclusion, regulatory T-cells, most notable EOMES$^+$Tr1-like cells, produce high amounts of IL-10 in PwMS, in particular in the CSF.

Regulatory T-cells in PwMS respond poorly to myelin antigens but are activated by EBV to produce IFN-γ and IL-10.

Antigenic activation induces T-cell proliferation and IL-10 production. We therefore analyzed if regulatory T-cells in MS patients were activated by a panel of self- and viral antigens that we showed previously activate CSF-infiltrating CD4$^+$T-cells in PwMS[50]. Since cytotoxic effector and regulatory T-cells proliferate poorly, we established an assay that enabled us to reproducibly detect also low frequencies (<1:10.000) of antigen-specific T-cells in PBMC *ex vivo,* independently of proliferation (sFigure 4). We detected overall weak IFN-γ T-cell responses to myelin-derived antigens (Figure 4A), but CD8$^+$T-cells and Th-cells showed nevertheless statistically significant responses in respectively untreated and Natalizumab-treated PwMS as compared to the no peptide control (sFigure 5A). Importantly, EOMES$^+$Tr1-like cells largely failed to respond at all to myelin-derived antigens, including MOG, MBP and PLP (Figure 4A and sFigure 5A, B). In marked contrast, we detected significant IFN-γ responses to EBV, i.e. to a pool of immunodominant peptides derived from 15 different EBV proteins, of EOMES$^+$Tr1-like cells in HD and PwMs (Figure 4A, sFigure 5A). Importantly, Th-cells and in particular EOMES$^+$Tr1-like cells responded strongly to EBV in Natalizumab-treated PwMS. Conversely, CD4$^+$CTL and CCR6$^+$GzmK$^+$ subsets responded poorly or not at all. CD8$^+$T-cells showed a very strong response to EBV that was further increased in PwMS, independently of Natalizumab treatment (sFigure 5A). T-cell responses to JCV, a persistent virus that may cause progressive multifocal leukoencephalopathy (PML) upon Natalizumab therapy, showed a completely different pattern. Thus, JCV activated predominantly Th-cells and CD4$^+$CTL, but only weakly CD8$^+$T-cells. EOMES$^+$Tr1-like cells responded weakly or not at all. JCV-specific CD4$^+$T-cell responses were significantly reduced in treatment-naïve PwMS, but not in Natalizumab-treated patients, as compared to HDs (Figure 4A, sFigure 5A).

Interestingly, we also detected some IFN-γ production by FOXP3$^+$Tregs in response to EBV (Figure 4A). Since only a minority of FOXP3$^+$Tregs can produce IFN-γ (Figure 3D), we analysed antigen-specific Treg responses according to 4-1BB induction (Figure 4B)[41]. FOXP3$^+$Tregs showed a weak EBV-specific response in HDs but responded strongly and significantly in Natalizumab-treated PwMS. Responses of FOXP3$^+$Tregs to myelin-derived antigens and JCV were in contrast weak.

The strong increase of EBV-specific CD4$^+$T-cells in Natalizumab-treated patients suggested that they could migrate to the CNS. Indeed, we showed previously that CSF-derived Th1-cell lines of PwMS responded efficiently to EBV[27,50]. EOMES expression in EOMES$^+$Tr1-like cells is stably maintained upon *in vitro* expansion[17], and here we found that a relevant fraction of CSF-derived CCR6$^-$CXCR3$^+$T-cells expressed EOMES (sFigure 5C), suggesting that they contained both EOMES$^-$Th1- and EOMES$^+$Tr1-like cells. Importantly, Eomes$^+$ cells showed a strong and significant IFN-γ response to EBV-derived peptides (Figure 4C), whereas EOMES$^-$ cells in the same CSF-derived lines responded significantly weaker.

EBV establishes a persistent, predominantly latent infection in B-cells, but can switch to lytic infection that leads to the expression of several immunogenic proteins[14]. In Natalizumab-treated PwMS, EOMES$^+$Tr1-like cells were strongly activated by a peptide pool of EBNA1 (Figure 4D, sFigure5D), the most consistently expressed viral protein in latently infected cells. Notably, in a patient that donated enough blood to sort EOMES$^+$Tr1-like cells, we observed also a strong proliferative response to EBNA1 (sFigure5E). In marked contrast, EOMES$^+$Tr1-like cells responded poorly to two immunogenic lytic antigens (BZLF1 and BMRF1 (Figure 4D, sFigure 5D, F). Interestingly, Th-cells, CD8$^+$T-cells and FOXP3$^+$Tregs responded in contrast also to these lytic EBV antigens, in particular in Natalizumab-treated patients (sFigure 5D).

We then investigated if EBV-specific T-cells could produce IL-10. We detected significant IL-10 production by EOMES$^+$Tr1-like cells in response to the immunodominant EBV peptide pool and to EBNA1, whereas IL-10 was undetectable with myelin-derived antigens (Figure 4E). Similar results were obtained with FOXP3$^+$Tregs. Conversely, no significant IL-10 responses were detected in Th-cells (sFigure 5G).

To understand if EBNA1-specific regulatory T-cells may be a unique feature of MS, we finally analyzed patients with systemic lupus erythematosus (SLE), a systemic autoimmune disease that is also associated with EBV and may affect the CNS. Interestingly, EOMES$^+$Tr1-like cells and FOXP3$^+$Tregs showed increased responses when challenged with the EBV peptide pool in

SLE patients with CNS involvement as compared to SLE patients without (Figure 4F, sFigure 5H, I). However, they failed to respond to EBNA1.

In conclusion, regulatory T-cells, particularly EOMES$^+$Tr1-like cells, are activated by the latency-associated EBV-derived antigen EBNA1 in PwMS to produce IFN-γ and IL-10 but largely fail to respond to myelin-derived antigens.

EBNA1-specific EOMES$^+$Tr1-like cells are associated with anti-EBNA1 IgG in PwMS and are hardly detectable following therapeutic B-cell depletion.

Anti-EBNA1 IgG antibody levels represent a strong independent environmental risk factor for MS[26]. Consistently, anti-EBNA1 IgG were significantly increased in PwMS compared to HD (sFigure 6A). EBNA1-specific CD4$^+$T-cells were significantly associated with EBNA1 IgG serum levels in PwMS treated with Natalizumab (Figure 5A), which retains CNS-homing T-cells in the blood. This was also true for EBNA1-specific EOMES$^+$Tr1-like cells (sFigure6B), and most prominent for IL-7R^{lo}EOMES$^+$Tr1-like effector cells (Figure 5A). Conversely, no significant association was observed with EBNA1-specific FOXP3$^+$Tregs. Surprisingly, there was also no association with EBNA1-specific Th-cells, in spite of the fact that predominantly the latter upregulated CD40L (Figure 5B), which is required for IgG induction from B-cells[51].

We next asked if the generation of EBNA1-specific EOMES$^+$Tr1-like cells was influenced by the major genetic risk factor of MS, the MHC class II allele HLA-DRB1*15, which could present critical peptides to activate CD4$^+$T-cells[52]. As expected, HLA-DR15$^+$ individuals were enriched among the Natalizumab-treated PwMS (9 of 24, Table 3). HLA-DR15$^+$ and HLA-DR15$^-$ patients showed similar CD4$^+$Th- and CD8$^+$T-cell IFN-γ responses to the immunodominant peptide pool of EBV (Figure 5C). Interestingly, EOMES$^+$Tr1-like cells showed in mean stronger responses to EBV- and EBNA1-derived peptides in HLA-DR15$^+$ patients, but individual responses were highly variable, and the increases did not reach statistical significance. Also Tregs and Th-cells responded in mean stronger to EBNA1 in HLA-DR15$^+$ patients, while CD8$^+$T-cells responded poorly (Figure 5C), but these differences did again not reach statistical significance. Finally, EBV/EBNA1-induced IL-10 production by EOMES$^+$Tr1-like cells was not increased in PwMS with the risk haplotype (sFigure 6C).

We then asked if EBV-specific regulatory T-cells were affected by Ocrelizumab, a therapeutic antibody that depletes B-cells, which could present EBV-derived antigens to T-cells. Indeed, a cohort of Ocrelizumab-treated patients (Table 1) had strongly and significantly reduced

CD8$^+$T-cell responses to EBV as compared to a control cohort of untreated PwMS, suggesting an ongoing T-cell activation by EBV-infected B-cells in MS. Intriguingly, among CD4$^+$T-cells only EBV/EBNA1-specific EOMES$^+$Tr1-like cells were significantly reduced, and they were in most cases even undetectable (Figure 5D). In contrast, EBV/EBNA1-specific Th-cells and FOXP3$^+$Tregs were detectable in most Ocrelizumab-treated patients. FOXP3$^+$Tregs were not reduced, whereas Th-cells were partially, but not significantly reduced (Figure 5D).

In conclusion, EBNA1-specific EOMES$^+$Tr1-like cells are associated with anti-EBNA1 IgG, tend to be more efficiently generated in patients with the HLA-DR15 risk haplotype and disappear following therapeutic B-cell depletion.

Table 3: HLA-DRB1 polymorphisms of Natalizumab-treated PwMS

Patient	1	2	3	4	5	6	8	9	10	11	12	13	14	15	16	17	18	19	20	21	22	23	24
HLA-DR1	11	01	11	13	04	13	03	11	11	15	13	11	11	01	11	11	04	07	11	15	04	11	11
HLA-DR2	11	08	13	13	11	15	11	13	15	16	15	11	12	11	16	13	11	15	15	16	15	16	15

EOMES$^+$Tr1-like cells produce IL-10 in brain lesions of PwMS.

Finally, to assess if EOMES$^+$Tr1-like cells can infiltrate the CNS of PwMS, postmortem brain sections of P-MS cases were stained for CD4, EOMES and IL-10 (Figure 6, sFigure 7). EOMES$^+$IL-10$^+$CD4$^+$ cells were identified in three different MS cases. They were found in the perivascular infiltrates of one active and one chronic active white matter lesion (Figure 6A, D-F) and in the inflamed meninges (Fig. 6H and insets). Cells co-expressing CD4 and EOMES, but not IL-10, were more frequently detected (brown/red arrows in Figure 6A, H). They could represent either pro-inflammatory cells[38] or EOMES$^+$Tr1-like cells that were not activated to produce IL-10. EOMES was also detected in CD4$^-$IL-10$^-$ cells (brown arrows in Figure 6A, H), and double staining of serial brain sections with anti-CD8 and anti-EOMES antibodies revealed the presence of EOMES$^+$CD8$^+$ cells in the same areas (Figure 6, inset in I).

CD4$^+$ and CD4$^-$ cells expressing IL-10, but not EOMES, were also detectable (Figure 6, insets in H). To estimate the relative abundance of CNS-infiltrating EOMES$^+$IL-10$^+$CD4$^+$Tr1-like cells, cells were counted in the brain sections. Approximately half of the IL-10$^+$ cells expressed CD4. CD4$^+$IL-10$^+$EOMES$^+$Tr1-like cells represented 6,3$\pm$3% (mean $\pm$ SD) of total CD4$^+$T cells without any appreciable difference between meningeal and parenchymal inflammatory cell infiltrates.

The percentages of CD4$^+$ cells expressing either EOMES or IL-10 alone were more variable (EOMES$^+$: 14±10%; IL-10$^+$: 3.3±3.8%, respectively), but did again not differ significantly between meningeal and parenchymal immune infiltrates. No IL-10 immunoreactivity was detected in intraparenchymal neural cells and microglia. Immunostaining for CD20 (Figure 6C, J), and *in situ* hybridization for the non-coding EBV-derived RNA EBER (Figure 6G, K), performed in consecutive brain sections, revealed the presence of numerous B-cells and EBV-infected cells in the same immune infiltrates that contained EOMES$^+$Tr1-like cells.
Overall, this analysis indicates that EOMES$^+$Tr1-like cells are present in the MS brain, some in the vicinity of CD8$^+$T-cells and EBV-infected B-cells and are locally activated to produce IL-10.

Discussion

Eomes$^+$CD4$^+$T-cells contain highly pro-inflammatory subsets, and have been proposed to play a pathogenic role in EAE[37] and in progressive MS[38]. Our findings point to a prominent role of anti-inflammatory EOMES$^+$Tr1-like cells in MS. Thus, we documented here a dysregulated homeostasis of EOMES$^+$Tr1-like cells in MS that was related to their recruitment and activation in the CNS, resulting in IL-10 production and proliferation. We further showed that these adaptive regulatory T-cells could be activated by EBNA1 to produce IL-10, but not by myelin-derived antigens.
At variance with previous reports on defective IL-10 production by CD4$^+$T-cells in MS[33,36], and by our group in Inflammatory Bowel Diseases[46], we found that EOMES$^+$Tr1-like cells produced high amounts of IL-10 in PwMS, and that they were the major IL-10 producing T-cell subsets in the CSF and also in the MS brain. IL-10 is known to exert anti-inflammatory functions in the CNS[53]. However, also a role for T-cell derived IL-10 in sustaining pathogenic T cell survival and CNS inflammation in EAE was recently reported[54]. In addition to IL-10, EOMES$^+$Tr1-like cells produce high levels of IFN-γ, but the latter has a neutral or even protective role in CNS inflammation[35,55]. EOMES$^+$Tr1-like cells may however release cytotoxic molecules that could cause collateral CNS damage[56].

IL-10 production and proliferation of adaptive regulatory T-cells are controlled by T-cell receptor stimulation. Therefore, the identification of the antigens that generate and activate these cells is a key issue to understand their functions, in particular in MS[50]. In the EAE model, T-cells, including adaptive regulatory T-cells, are deliberately primed by myelin-derived self-

antigens. Conversely, we showed here that regulatory T-cells largely failed to respond to three major CNS autoantigens in PwMS. The failure to suppress myelin-targeted autoimmunity may explain the extensive CNS damage in MS. An unexpected key finding of this study is that regulatory T-cells in MS are activated by EBV, a persistent virus that has an essential, but also still enigmatic[30], role in MS pathology[57]. EOMES$^+$Tr1-like cells responded selectively to EBNA1, the viral protein that is most consistently expressed in latently infected B-cells, and therefore represents the virus' Achilles heel[14]. Notably, responses to EBNA1 in PwMS were previously reported for Th1-cells[58], but since markers of EOMES$^+$Tr1-cells were identified only later, these IFN-γ-producing CD4$^+$T-cells contained probably both conventional Th1-cells and EOMES$^+$Tr1-like cells. Here we showed that EBNA1-specific EOMES$^+$Tr1-like cells were characteristic for MS but were not detectable in SLE patients with CNS involvement and are thus likely to represent a MS-associated viral evasion strategy. Antibodies and T-cells that cross-react with EBNA1 and epitopes from self-proteins have been identified in PwMS[27,52,58,59], suggesting that EBV infection might promote MS pathology through molecular mimicry. EOMES$^+$Tr1-like cells failed however to respond to the three major myelin-derived antigens. Consistently, EBNA1-specific CD4$^+$T-cells that cross-reacted with myelin-derived antigens were a minor fraction and produced IL-2, but not CCL4[58], indicating that the cross-reactive cells were conventional Th1-cells, but not EOMES$^+$Tr1-like cells. We can of course not exclude that EOMES$^+$Tr1-like are activated by other cross-reactive antigens[52], but molecular mimicry leading to the activation of regulatory T-cells would be expected to have a paradoxical beneficial effect.

EOMES$^+$Tr1-like cells lack B-cell helper functions and may suppress T-cell-dependent B-cell responses unless they up-regulate CD40L[60]. Since also EBNA1-specific EOMES$^+$Tr1-like cells in MS failed to up-regulate CD40L, it seems unlikely that they activate B-cells to produce anti-EBNA1 IgG antibodies. The association of EBNA1-specific IgG and EOMES$^+$Tr1-like cells could however reflect antigen presentation by EBNA1-specific B-cells, which can internalize EBNA1 via their BCRs with very high efficiency to present EBNA1-derived epitopes on MHC Class-II to CD4$^+$T-cells[61]. Consistently, EBNA1-specific EOMES$^+$Tr1-like cells disappeared from the CD4$^+$T-cell compartment upon therapeutic B-cell depletion. Anti-EBNA1 antibodies may promote MS by molecular mimicry. Nevertheless, it is also possible that EBNA1-specific B-cells increase the risk of MS because they induce EBNA1-specific regulatory T-cells that allow viral immune

escape. EBNA1-specific regulatory T-cells are expected to inhibit the killing of latently infected B-cells[62]. CXCR3-dependent homing of the surviving EBV-infected B-cells to the CNS[63] could then trigger the recruitment of virus-specific T-cells[64-70] and of auto-reactive Th1/17 bystander cells[9,69,70], leading ultimately to CNS damage[27]. In this scenario EBV-specific regulatory T-cells could have a net detrimental role in MS, although IL-10 produced by EOMES$^+$Tr1-like cells could transiently dampen CNS inflammation.

CD8$^+$T-cell responses to EBV are of broader magnitude in PwMS, but they recognise predominantly lytic antigens[71], suggesting that immune surveillance of latently infected B-cells may be inefficient. Indeed, increased EBV reactivation and CD8$^+$T-cell responses to lytic EBV antigens have been associated with active MS[68]. Moreover, immune-deficient mice reconstituted with human immune cells from HLA-DRB1*15:01-positive individuals had an inefficient control of EBV infection and mount dysregulated EBV-specific CD8$^+$T-cell responses[72], providing a link between the HLA risk haplotype and an inefficient EBV immune control. Interestingly, we detected relatively high, although variable, frequencies of EBV-specific regulatory T-cells and low EBNA1-specific CD8$^+$T-cell responses in HLA-DR15$^+$ patients. The fact that EBNA1-specific Tr1-like cells are present also in HLA-DR15$^-$ PwMS indicates that EBNA1-derived epitopes that induce EOMES$^+$Tr1-like cells are not exclusively HLA-DR15-restricted. Finally, studies in post-mortem brain tissue from PwMS suggested that EBV, which could be detected in B-cell enriched inflammatory infiltrates in the CNS in PwMS in some patients, could lead to the recruitment and activation of EBV-specific CD8$^+$T-cells[69,73]. Our finding that EOMES$^+$Tr1-like cells were present in the same CNS inflammatory infiltrates where EBV$^+$B-cells and CD8$^+$T-cells were detectable supports the concept that EOMES$^+$Tr1-like-cell could inhibit EBV-specific immune responses in the CNS. Indeed, EOMES$^+$Tr1-like cells and FOXP3$^+$Tregs can suppress CD8$^+$T-cell responses[17,22]. Thus, the MS-associated EBV-specific regulatory T-cells are expected to inhibit CD8$^+$T-cell-dependent immune surveillance of EBV, in particular of latently infected B-cells[66,68,69,71,72,74]. This in turn could promote the generation of EBNA1-specific EOMES$^+$Tr1-like cells due to persistent antigenic stimulation in a positive feed-forward loop. EBV-specific regulatory T-cells may thus be both the cause and the consequence of an inefficient anti-EBV immune control in PwMS. Although the precise mechanism how EBV exerts its detrimental role in MS is debated, our data suggests that EBV-specific regulatory T-cells are likely to play in any case a key role.

A lack of protection by regulatory T-cells is assumed to be associated with reduced Treg numbers or functions, namely IL-10 production in MS. Our findings suggest the novel concept that Treg dysfunction may also be a consequence of an aberrant antigen specificity, which promotes immune evasion of a disease-associated pathogen but is suboptimal to inhibit auto-reactive T-cells and tissue damage. A general implication of this study is further that the analysis of polyclonal adaptive Treg populations without the knowledge of their antigen specificities may be insufficient to understand their role in complex human pathologies.

Acknowledgments:

This work was supported by FISM - Fondazione Italiana Sclerosi Multipla (2017/R/14) and co-financed with the '5 per mille' public funding. This project has received also funding from the European Union's Horizon Europe Research and Innovation Actions under grant no. 101137235 (BEHIND-MS). Views and opinions expressed are however those of the author(s) only and do not necessarily reflect those of the European Union nor the granting authority. Neither the European Union nor the granting authority can be held responsible for them. JG is supported by AIRC (IG 20385). DG and ES are supported by the Italian Ministry of Health (Ricerca Corrente). We thank Manuel Albanese and Samuele Nortabartolo for critical reading and comments, and Francesca Aloisi for inspiring discussion and suggestions.

Table 1: Characteristics of PwMS and healthy donors

Table 2: Characteristics of SLE patients with and without CNS involevment

Table 3: HLA-DRB1 polymorphisms of Natalizumab-treated PwMS

sTable 1: Differentially expressed genes in Cluster 1-13

sTable 2: Differentially expressed genes in EOMES$^+$Tr1-like cells versus CCR6$^+$GzmK$^+$ cells

sTable 3: Differentially expressed genes in EOMES$^+$Tr1-like cells: CSF versus blood

sTable 4: Flow Cytometry antibody panels

Figure Legends

Figure 1: Dysregulated Homeostasis of EOMES$^+$Tr1-like effector cells in PwMS

A. UMAP of T-cell clusters identified in peripheral blood of treatment-naïve RR-PwMS (n=14) and healthy donors (n=12) by multiparametric flow cytometry. Clusters are identified by numbers, different colors and named as indicated in the panel**. B.** Frequencies of Tr1-like effector cells (CD4$^+$GzmK$^+$IL7R^{lo}) among CD4$^+$T-cells in HDs, untreated P-PwMS, treatment-naïve and Natalizumab-treated RR-PwMS. **C.** VLA-4 expression on CD4$^+$T-cell subsets in treatment-naive RR-MS patients (n=4) and HDs (n=9). **D.** Ki67 expression of Tr1-like effector cells in HDs, untreated P-PwMS, treatment-naïve and Natalizumab-treated RR-PwMS. **B/D.** HDs n=35, P-PwMS n=3, treatment-naïve RR-PwMS n=11, Natalizumab-treated RR-PwMS n=20. **B-D.** Statistical significance was calculated by One-way ANOVA.

Figure 2: EOMES$^+$Tr1-like cells generate a distinct cluster among single-sequenced CD4$^+$T-cells and are enriched in the cerebrospinal fluid of PwMS

A. UMAP of 13 antigen-experienced T-cell clusters in the blood and the CSF of 4 PwMS and 4 control donors. **B.** Gene Set Enrichment Analysis of reference EOMES$^+$Tr1-like signature genes of Cluster 7 (Overlay of all conditions). The enrichment score (ES) and its p-value are reported in the panel. **C.** UMAPs of the indicated EOMES$^+$Tr1-like signature genes in the CSF of PwMS. **D.** Heatmap of CCR6, GzmK and IL-7R expression in the 13 clusters (Overlay of all conditions). **E.** Heatmap of selected differentially expressed genes of Cluster 7 (EOMES$^+$Tr1-like), 11 (CCR6$^+$GzmK$^+$) and 13 (FOXP3$^+$Tregs). Relative average expression levels in the CSF and in the blood in PwMS and control individuals are shown. **F.** Frequencies of Cluster 7 (EOMES+Tr1-like) and 11 (CCR6$^+$GzmK$^+$) in the blood and the CSF of PwMs and control donors. **G** Frequencies of the indicated CD4$^+$T-cell subsets in peripheral blood (PB, n=17) and the cerebrospinal fluid (CSF, n=5) of treatment-naïve PwMS were assessed by flow cytometry. Statistical significance was calculated with an unpaired t-test. **H**. CXCR3 protein expression in the indicated CD4$^+$T-cell subsets in peripheral blood (PB, n=11) and in the CSF of PwMS (n=3). Statistical significance was calculated by One-way ANOVA.

Figure 3: EOMES$^+$Tr1-like cells produce high levels of IL-10 in the CSF of PwMS

A. UMAPS showing scaled gene co-expression of IL-10 with GzmK (left) or FOXP3 (right). The colour code and the relative scaled co-expression levels are reported in the panel. **B-E.** T-cells

in PB and the CSF of untreated PwMS or HDs were activated with PMA and Ionomycin and analyzed for the expression of cytokines and differentiation markers. **B/C.** Clusters were identified and indicated by numbers, colors and names as indicated in the panel**. B.** Relative contributions of the 10 identified clusters to $CD4^+$T-cells in PB and CSF **C.** Diffusion map analysis of the same clusters in PB and CSF predicting differentiation relationships in pseudotime. **D/E.** Analysis of cytokine production by $CD4^+$T-cell subsets in the blood of HDs (n=19) and in the blood and the CSF of PwMS (n=4). **D.** IL-10 and IFN-γ production by the indicated $CD4^+$T-cell subsets. Statistical significance was calculated by 2-way ANOVA **E.** Pie charts illustrating the relative contributions of the indicated T-cell subsets to the pool of IL-10-producing $CD4^+$T-cells. Color code and mean percentages are reported in the panel. Statistical significance between PB and CSF of PwMS was calculated with an unpaired t-test.

Figure 4: EOMES+Tr1-like cells are selectively activated by the EBV antigen EBNA1 in PwMS. **A.** Peripheral blood mononuclear cells were stimulated with peptide pools derived from MOG plus MBP, EBV (immunodominant pool) or JCV (VP1/2). T-cell subsets were tracked according to differentiation markers, and antigen-specific cells identified by CD69 upregulation and IFN-γ production (sFigure 4). Frequencies of antigen-specific cells in the indicated subsets are shown as stacked histograms among total $CD4^+$T-cells, according to the indicated color code. Antigen-specific responses were analysed in HDs (MOG/MBP n=12, EBV n=24 and JCV n=10), treatment-naive (n=9, 10 and 8) and Natalizumab-treated PwMS (n=20, 27 and 16). **B.** Antigen-specific Tregs were tracked according to 4-1BB and/or IFN-γ expression among $CD69^+$Tregs (HD n=10-24, untreated RR-PwMS n=2-5, Natalizumab-treated RR-PwMS n=10-15). **C.** CSF-derived $CXCR3^+CCR6^-$Th-cell lines from 5 treatment-naive MS patients were stimulated with EBV or MOG/MBP-derived peptides, and IFN-γ production in gated $EOMES^+$ and $EOMES^-$ cells analysed. **D.** Antigen-specific IFN-γ responses to overlapping peptide pools derived from EBNA1 and BZLF1 (HD: n=9,6; untreated RR-PwMS: n=6; Natalizumab-treated RR-PwMS: n=26,14). **E.** IL-10 production by EOMES+Tr1-like cells and $FOXP3^+$Tregs in response to EBV (immunodominant pool) or EBNA1 (n=16) or MOG plus MBP (n=5) in Natalizumab-treated PwMS. **F.** Antigen-specific IFN-γ responses in SLE patients with (n=6) or without (n=11) CNS involvement to EBV (upper panel) or EBNA1 (lower panel).

Figure 5: EBNA1-specifc EOMES$^+$Tr1-like cells are associated with anti-EBNA1 IgG levels and disappear in Ocrelizumab-treated patients.

A. The frequencies of EBNA1-specific CD4$^+$T-cells, Th-cells, EOMES$^+$IL-7R^{lo}Tr1-like effector cells and FOXP3$^+$Tregs in Natalizumab-treated patients (n=11-19) were plotted against the serum levels of anti-EBNA1 IgG antibodies. R and p-values are reported on the right of the panels. **B.** CD40L expression of CD4$^+$T-cell stimulated with EBV- or EBNA1-derived peptides T-cells (n=13) is shown. Statistical significance of CD40L expression of Th-cells versus Tr1-cells and Tregs was calculated by two-way Annova. **C.** Natalizumab-treated PwMS were HLA-haplotyped (Table 3) and T-cell responses stratified according to the expression of HLA-DRB1*15 (DR15$^+$(n=5-9), DR15$^-$ (n=11-14)). **D.** EBV-specific T-cell response in untreated (n(RR,P)=10,3) and Ocrelizumab-treated PwMS (n(RR,P)=6,11)). **C/D.** Shown are responses of the indicated EBV-reactive CD4$^+$T-cell subsets and of total CD8$^+$T-cells to EBV (immunodominant pool, upper panels) and to EBNA1 (lower panels). Statistical significances were calculated with an unpaired t-test.

Figure 6: EOMES$^+$ Tr1-like cells produce IL-10 in MS brain lesions.

Triple immunostaining in bright field for EOMES (nuclear brown staining), IL-10 (blue) and CD4 (red) reveals presence of EOMES$^+$IL-10$^+$CD4$^+$Tr1-like cells in perivascular immune infiltrates in one active WM lesion (blue/red arrows in A, D-F) and in the inflamed meninges (H) of one MS donor. In the same infiltrates, CD4$^+$ cells expressing only EOMES (red/brown arrow in A and H), EOMES$^-$IL-10$^-$CD4$^+$ cells (red arrow in A) and EOMES$^+$IL-10$^-$CD4$^-$ cells (brown arrow in A and H) were also detected. Panels E and F, inset in D and the left insets in H show four EOMES$^+$IL-10$^+$CD4$^+$ cells at high power magnification. In the right inset in H, two EOMES$^-$IL-10$^+$ cells (arrows) one of which co-expresses CD4 (white arrow) are shown at high magnification. Immunostaining for CD8 (B and I) and double staining for CD8 and EOMES (inset in I), performed in serial sections, highlight the presence of numerous CD8$^+$T-cells, some of which express EOMES, in the same immune infiltrates shown in A and H. Immunohistochemistry for CD20 (C and J) and in situ hybridization for the small non-coding EBV RNA (EBER) (G, K), performed in consecutive sections, reveal substantial B-cell infiltration and the presence of EBV-infected cells in the same brain areas. Bars: 100 µm in B, C, I-K; 50 µm in G; 20 µm in A, D, H and insets in G and K; 10 µm in E, F and inset in D, right inset in H, and inset in I; 5 µm in the insets in H.

Supplementary Figures

sFigure 1: Multiparametric Flow cytometric analysis of T-cells from peripheral blood of HDs and PwMS.

A. Histograms showing the expression of the 18 markers analysed to classify T-cells from peripheral blood of HDs and of PwMS in the 27 identified T-cell clusters.

B. UMAP maps of the identified T-cell clusters showing the individual expression of the 15 most relevant markers.

C. Unsupervised hierarchical clustering of the 12 $CD4^+$T-cell clusters according to the expression of the indicated differentiation markers. Red indicates high and blue low expression.

D. Gating strategy to identify $FOXP3^+$Tregs (left), $GzmB^+$CTL, Th-cells (central panel) and $GzmK^+$ subsets (right panel), namely IL-$7R^{+/lo}$Tr1-like and $CCR6^+$ cells.

E. EOMES expression in the indicated T-cell subsets (n=9) in PwMS.

F. Cytokine profiles of $GzmK^+CD4^+$T-cell subsets in PwMS

G. Frequencies and **H.** Ki67 expression of the indicated major $CD4^+$T-cell subsets in 35HDs, 3 untreated P-PwMS, 11 treatment-naïve and 20 Natalizumab-treated RR-PwMS.

sFigure 2 Characterization of $EOMES^+$Tr1-like cells in the CSF of PwMS.

A. Dot plot showing expression levels of the indicated signature genes of central memory, Tfh, Th1, Th2, Th17, CTL, $EOMES^+$Tr1-like, Treg and IFN-activated cells in the 13 $CD4^+$T-cell clusters

B. UMAPS of individual signature genes of Tfh (CXCR5), IFN activate cells (IFIT3), Th2 (PTGDR2/CRTH2), C TL (GzmB) and Treg (FOXP3, overlay of all 4 conditions)

C. UMAPS of additional $EOMES^+$Tr1-like-associated genes (LAG3, ITGA2/CD49b, CTLA-4, HAVCR2/TIM3, overlay of all 4 conditions)

D. UMAPS (Overlay of all 4 conditions) of GzmK and of the indicated Th1/17-associated genes (CCR6, RORC, IL-23, IL-18RAP)

E. Heatmaps showing the average expression of genes upregulated in CSF-infiltrating versus circulating $EOMES^+$Tr1-like cells involved in Cholesterol metabolism and selectively down-regulated gens in $EOMES^+$Tr1-like cells (upper) and all other $CD4^+$T-cells (lower panel) in the CSF and in the blood-

F. Relative contributions of the identified clusters to total antigen-experienced $CD4^+$T-cells in the blood and the CSF of PwMS and control Donors.

G. CXCR3 surface expression on the indicated $Ki67^+$ T-cell subsets in treatment-naïve RR-PwMS (n=7-11).

sFigure 3 Cytokine profiles of $CD4^+$T-cell subsets.

A. UMAPs showing the scaled co-expression of IL-10, IFN-γ and IL-2 with IL-7R. Color code and relative scaled co-expression levels are reported in the panel.

B. Hierarchical clustering of the 10 identified $CD4^+$ T-cell clusters according to the expression of cytokines and differentiation markers in the blood and CSF of active MS patients.

C. Diffusion Maps showing the expression of 7 principal markers that characterize the cytokine producing T-cell clusters.

D. IL-10 and IFN-γ production by $EOMES^+$Tr1-like cells in HDs (n=19) and RR- (n=2-3) or P-PwMS (PB n=2) in the blood or the CSF.

sFigure 4: Gating strategy to track antigen-specific T-cells *ex vivo.*

A. TCR-induced T-cell responses identified by concomitant CD69 and IFN-γ induction in gated $CD4^+$T-cells.

B. TCR-induced responses of $FOXP3^+$Tregs identified by concomitant CD69 and 4-1BB induction.

C. TCR-induced upregulation of CD40L versus IL-10 on total $CD4^+$T-cells.

A-C. Shown are the negative (Ctr-, no antigen) and the positive (Ctr+, super-antigen SEB) control.

D. Stable expression of subset-specific markers in unstimulated (Ctr-) and SEB-stimulated (Ctr+) $CD4^+$T-cells

E. 3 HDs were stimulated with or without the immunodominant pool of EBV peptides (EBV) and EBV-specific T-cells analysed. Shown are 3 technical triplicates for each donor to document reproducibility.

sFigure 5 Analysis of T-cell antigen specificities.

A. Antigen specificities of T-cell subsets. Reported are frequencies $CD69^{+}IFN\text{-}\gamma^{+}$ cells in individual $CD4^{+}FOXP3^{-}$T-cell subsets among $CD4^{+}$T-cells and responses in total $CD8^{+}$T-cells in HDs (n=10-21), in untreated (n=10-14) and Natalizumab-treated PwMS (n=17-20). Left panels show responses following stimulation with overlapping peptide pools of MOG and MBP, central panels to an immunodominant peptide pool derived from EBV or and right panels to overlapping peptide pools of VP1 and VP2 from JCV. Squares on top of columns indicate statistical significances as compared to the no peptide control. Stars on top of lines indicate statistical significances between different cohorts.

B. Lack of responses of $GzmK^{+}$T-cell subsets, i.e. frequencies of $CD69^{+}IFN\text{-}\gamma^{+}$ cells in the indicated subset among total $CD4^{+}$T-cells, to PLP (6 HDs and 6 Natalizumab-treated MS patients)

C. $CD4^{+}CXCR3^{+}CCR6^{-}$"Th1" and $CXCR3^{-}CCR6^{+}$"Th17" cell lines derived from the CSF from 5 different treatment-naïve MS patients were analysed for EOMES expression. Shown are the mean percentages of $EOMES^{+}$ cells, and the p-value is indicated.

D. Responses of the indicated T-cell subsets to individual EBV-derived antigens, namely EBNA1, BZLF1 and BMRF1 in HDs (EBNA1: n=9, BZLF1: n=6, BMRF1: n=7), untreated ("MS", EBNA1: n=9, BZLF1: n=8, BMRF1: n=3 and Natalizumab-treated PwMS ("+NTZ" EBNA1: n=19, BZLF1: n=17, BMRF1: n=11). Responses of $FOXP3^{+}$Tregs (HD: n=7, MS n=3, +NTZ: n=11) were assessed according to 4-1BB induction and IFN-γ production, all other subsets according to CD69 up-regulation and concomitant IFN-γ production. Squares on top of columns indicate statistical significances as compared to the no peptide control. Stars on top of lines indicate statistical significances between different cohorts.

E. Sorted Tr1-like cells ($CD4^{+}CCR5^{+}CD27^{+}CCR6^{-}CD25^{-}$), Th1-cells ($CD4^{+}CXCR3^{+}CCR6^{-}CCR5^{-}CD25^{-}$) or Tregs ($CD4^{+}CD25^{+}IL\text{-}7R^{lo}$) were labelled with CellTrace, stimulated with autologous monocytes and EBNA1 peptides and proliferation and CD25 expression analysed after 7 days.

F. Stacked histograms showing responses of $CD4^{+}$T-cell subsets to the lytic EBV antigen BMRF1 in HDs (n=10), treatment-naïve (n=2) and Natalizumab-treated PwMS (n=13).

G. IL-10 production by Th-cells in response to EBV, EBNA1 and MOG/MBP in Natalizumab-treated PwMS (n=12).

H. IFN-γ responses of peptide-activated $CD4^+GzmK^+$T-cell subsets, $CD4^+$CTL, Th-cells and $FOXP3^+$Tregs to EBV and EBNA1 in SLE patients without (n=11) or with (n=6) CNS involvement ("+ CNS").

I. IL-10 production in EBV and EBNA1-activated $EOMES^+$Tr1-like cells and by $FOXP3^+$Tregs in SLE patients with and without CNS involvement.

sFigure 6 Associations of EBNA1-specific T-cells with MS risk factors.

A. Anti-EBNA1 IgG serum levels in HDs (n=15) and MS patients (untreated: n=15, Natalizumab-treated: n=21).

B. Plot illustrating the association of total ($IL\text{-}7R^{+\text{ and lo}}$) EBNA1-specific Tr1-like cells with anti-EBNA1 IgG levels. R- and p-values are indicated.

C. IL-10 production by $EOMES^+$Tr1-like cells and $FOXP3^+$Tregs, in response to EBV and EBNA1 in HLA-DR15+ and HLA-$DR15^-$ PwMS.

sFigure 7 Negative control for EOMES and IL-10 staining in brain sections.

Triple immunohistochemistry in bright field of MS brain tissue stained with 5 µg/ml purified rat IgG1 k isotype control (eBRG1), 5 µg/ml purified mouse IgG1k isotype control (P3.6.2.8.1) (both by Thermo Fisher Scientific) and rabbit monoclonal antibody to CD4, performed as described. Only immunoreactivity for CD4+ cells (red) was observed. Bar = 100 µm

Supplementary Material and Methods

Tissue processing and immunohistochemistry

Four tissue blocks from 4 MS cases were fixed in 4% paraformaldehyde (PFA), frozen and stored at -80°C until use (FF tissues); one tissue block from MS 330 case was formalin-fixed and paraffin embedded (FFPE). FFPE Acetone post-fixed FF tissue sections were air dried for 10 min at room temperature (RT); FFPE sections were dewaxed in xylene and rehydrated in decreasing series of ethanol. FF and FFPE sections were subjected to antigen retrieval treatment, in microwave with citrate buffer ph=6, permeabilization step with 0,5% Triton X100 in in phosphate buffered saline (PBS) for 10 minutes and blocking of endogenous peroxidase in 0.15% and 0.3% H_2O_2 in PBS, respectively. After incubation overnight (ON) at 4°C with anti-EOMES mouse mAb (clone WD1928, Thermo Fisher Scientific, Rockford, USA) diluted 1:50 in PBS containing 0.1% Triton X and 2% bovine serum albumin, sections were incubated for 1

hour with biotin-conjugated goat anti-mouse Ig (Jackson ImmunoResearch Laboratories, Cambridgeshire, UK) diluted in PBS + 2% normal goat serum (NGS), and then with avidin-biotin complex (ABC) (Vector Laboratories Inc., Burlingame, CA, USA) for 30 min. Immune-complexes were visualized with 3,3'-diaminobenzidine tetrahydrochloride (DAB, Sigma Aldrich, St. Louis, MO, USA; brown color). Then, after treatment with avidin-biotin blocking kit (Vector lab), the same sections were incubated ON at 4°C with rat anti-IL-10 mAb (clone JES3-9D7, Thermo Fisher Scientific; 1:100 diluted) and, the next day, after washing in PBS, with anti-CD4 rabbit mAb (clone QR032, Quartett, Postdam, Germany; 1:100 diluted) for 1 hour at RT. After washing in TBS, sections were treated sequentially with: AP-Polymer anti-rabbit (Zytochem plus 2-step double stain, polymer kit; Zytomed Systems GmbH, Berlin, Germany) for 30 min, TBS, permanent AP Red Kit containing Levamisol (Vector Lab; red color) for 10-15 min, distilled water, TBS, biotin conjugated donkey anti-rat Ig (Jackson Lab), ABC and, finally, with permanent HRP Green Kit (Zytomed Systems; green/blue colour). After very quick washing in distilled water, sections were sealed with Ultramount at 40°C for 30 min.

References

1. Sakaguchi, S.*, et al.* Foxp3+ CD25+ CD4+ natural regulatory T cells in dominant self-tolerance and autoimmune disease. *Immunological reviews* **212**, 8-27 (2006).
2. Ochs, H.D., Gambineri, E. & Torgerson, T.R. IPEX, FOXP3 and regulatory T-cells: a model for autoimmunity. *Immunologic research* **38**, 112-121 (2007).
3. Buckner, J.H. Mechanisms of impaired regulation by CD4(+)CD25(+)FOXP3(+) regulatory T cells in human autoimmune diseases. *Nat Rev Immunol* **10**, 849-859 (2010).
4. Suffia, I.J., Reckling, S.K., Piccirillo, C.A., Goldszmid, R.S. & Belkaid, Y. Infected site-restricted Foxp3+ natural regulatory T cells are specific for microbial antigens. *J Exp Med* **203**, 777-788 (2006).
5. Roncarolo, M.G.*, et al.* Interleukin-10-secreting type 1 regulatory T cells in rodents and humans. *Immunological reviews* **212**, 28-50 (2006).
6. Haringer, B., Lozza, L., Steckel, B. & Geginat, J. Identification and characterization of IL-10/IFN-gamma-producing effector-like T cells with regulatory function in human blood. *J Exp Med* **206**, 1009-1017 (2009).
7. Parish, I.A.*, et al.* Chronic viral infection promotes sustained Th1-derived immunoregulatory IL-10 via BLIMP-1. *The Journal of clinical investigation* (2014).
8. Gagliani, N.*, et al.* Antigen-specific dependence of Tr1-cell therapy in preclinical models of islet transplant. *Diabetes* **59**, 433-439 (2010).
9. Brockmann, L.*, et al.* Molecular and functional heterogeneity of IL-10-producing CD4(+) T cells. *Nat Commun* **9**, 5457 (2018).

10. Jankovic, D.*, et al.* Conventional T-bet(+)Foxp3(-) Th1 cells are the major source of host-protective regulatory IL-10 during intracellular protozoan infection. *J Exp Med* **204**, 273-283 (2007).
11. Jeon, S.G.*, et al.* Probiotic Bifidobacterium breve induces IL-10-producing Tr1 cells in the colon. *PLoS pathogens* **8**, e1002714 (2012).
12. Anderson, C.F., Oukka, M., Kuchroo, V.J. & Sacks, D. CD4(+)CD25(-)Foxp3(-) Th1 cells are the source of IL-10-mediated immune suppression in chronic cutaneous leishmaniasis. *J Exp Med* **204**, 285-297 (2007).
13. O'Garra, A. & Vieira, P. T(H)1 cells control themselves by producing interleukin-10. *Nat Rev Immunol* **7**, 425-428 (2007).
14. Murata, T.*, et al.* Molecular Basis of Epstein-Barr Virus Latency Establishment and Lytic Reactivation. *Viruses* **13**(2021).
15. Thelen, B.*, et al.* Eomes is sufficient to regulate IL-10 expression and cytotoxic effector molecules in murine CD4(+) T cells. *Front Immunol* **14**, 1058267 (2023).
16. Zhang, P.*, et al.* Eomesodermin promotes the development of type 1 regulatory T (TR1) cells. *Sci Immunol* **2**(2017).
17. Bonnal, R.J.P.*, et al.* Clonally expanded EOMES(+) Tr1-like cells in primary and metastatic tumors are associated with disease progression. *Nat Immunol* **22**, 735-745 (2021).
18. Geginat, J.*, et al.* Eomesodermin-expressing type 1 regulatory (EOMES(+) Tr1)-like T cells: Basic biology and role in immune-mediated diseases. *Eur J Immunol*, e2149775 (2023).
19. Gruarin, P.*, et al.* Eomesodermin controls a unique differentiation program in human IL-10 and IFN-gamma coproducing regulatory T cells. *Eur J Immunol* **49**, 96-111 (2019).
20. Dejean, A.S., Joulia, E. & Walzer, T. The role of Eomes in human CD4 T cell differentiation: A question of context. *Eur J Immunol* **49**, 38-41 (2019).
21. Mazzoni, A.*, et al.* Eomes controls the development of Th17-derived (non-classic) Th1 cells during chronic inflammation. *Eur J Immunol* (2018).
22. Pulvirenti, N.*, et al.* Characterization of human CD4(+) EOMES(+) GzmK(+) T-cell subsets unveils an uncoupling of suppressive functions from IL-10-producing capacities. *Eur J Immunol*, e2350675 (2024).
23. Gabrysova, L.*, et al.* Negative feedback control of the autoimmune response through antigen-induced differentiation of IL-10-secreting Th1 cells. *J Exp Med* **206**, 1755-1767 (2009).
24. Olsson, T., Barcellos, L.F. & Alfredsson, L. Interactions between genetic, lifestyle and environmental risk factors for multiple sclerosis. *Nat Rev Neurol* **13**, 25-36 (2017).
25. Wang, J.*, et al.* HLA-DR15 Molecules Jointly Shape an Autoreactive T Cell Repertoire in Multiple Sclerosis. *Cell* **183**, 1264-1281 e1220 (2020).
26. Bjornevik, K., Munz, C., Cohen, J.I. & Ascherio, A. Epstein-Barr virus as a leading cause of multiple sclerosis: mechanisms and implications. *Nat Rev Neurol* **19**, 160-171 (2023).
27. Geginat, J.*, et al.* The Enigmatic Role of Viruses in Multiple Sclerosis: Molecular Mimicry or Disturbed Immune Surveillance? *Trends Immunol* (2017).
28. Christensen, T. The role of EBV in MS pathogenesis. *Int MS J* **13**, 52-57 (2006).
29. Aloisi, F., Giovannoni, G. & Salvetti, M. Epstein-Barr virus as a cause of multiple sclerosis: opportunities for prevention and therapy. *Lancet Neurol* **22**, 338-349 (2023).

30. Kuchroo, V.K. & Weiner, H.L. How does Epstein-Barr virus trigger MS? *Immunity* **55**, 390-392 (2022).
31. Noori-Zadeh, A.*, et al.* Regulatory T cell number in multiple sclerosis patients: A meta-analysis. *Mult Scler Relat Disord* **5**, 73-76 (2016).
32. Carbone, F.*, et al.* Regulatory T cell proliferative potential is impaired in human autoimmune disease. *Nat Med* **20**, 69-74 (2014).
33. Sumida, T.*, et al.* Activated beta-catenin in Foxp3(+) regulatory T cells links inflammatory environments to autoimmunity. *Nat Immunol* **19**, 1391-1402 (2018).
34. Dominguez-Villar, M., Baecher-Allan, C.M. & Hafler, D.A. Identification of T helper type 1-like, Foxp3+ regulatory T cells in human autoimmune disease. *Nat Med* **17**, 673-675 (2011).
35. Heinemann, C.*, et al.* IL-27 and IL-12 oppose pro-inflammatory IL-23 in CD4+ T cells by inducing Blimp1. *Nat Commun* **5**, 3770 (2014).
36. Astier, A.L., Meiffren, G., Freeman, S. & Hafler, D.A. Alterations in CD46-mediated Tr1 regulatory T cells in patients with multiple sclerosis. *The Journal of clinical investigation* **116**, 3252-3257 (2006).
37. Stienne, C.*, et al.* Foxo3 Transcription Factor Drives Pathogenic T Helper 1 Differentiation by Inducing the Expression of Eomes. *Immunity* **45**, 774-787 (2016).
38. Raveney, B.J.E.*, et al.* Involvement of cytotoxic Eomes-expressing CD4(+) T cells in secondary progressive multiple sclerosis. *Proc Natl Acad Sci U S A* **118**(2021).
39. Peeters, L.M.*, et al.* Cytotoxic CD4+ T Cells Drive Multiple Sclerosis Progression. *Front Immunol* **8**, 1160 (2017).
40. Hartung, H.P., Graf, J., Aktas, O., Mares, J. & Barnett, M.H. Diagnosis of multiple sclerosis: revisions of the McDonald criteria 2017 - continuity and change. *Curr Opin Neurol* **32**, 327-337 (2019).
41. Schoenbrunn, A.*, et al.* A converse 4-1BB and CD40 ligand expression pattern delineates activated regulatory T cells (Treg) and conventional T cells enabling direct isolation of alloantigen-reactive natural Foxp3+ Treg. *Journal of immunology* **189**, 5985-5994 (2012).
42. Cossarizza, A.*, et al.* Guidelines for the use of flow cytometry and cell sorting in immunological studies (third edition). *Eur J Immunol* **51**, 2708-3145 (2021).
43. Serafini, B., Rosicarelli, B., Veroni, C. & Aloisi, F. Tissue-resident memory T cells in the multiple sclerosis brain and their relationship to Epstein-Barr virus infected B cells. *J Neuroimmunol* **376**, 578036 (2023).
44. Kendirli, A.*, et al.* A genome-wide in vivo CRISPR screen identifies essential regulators of T cell migration to the CNS in a multiple sclerosis model. *Nat Neurosci* **26**, 1713-1725 (2023).
45. De Simone, M.*, et al.* Ex vivo microRNA and gene expression profiling of human Tr1-like cells suggests a role for miR-92a and -125a in the regulation of EOMES and IL-10R. *Eur J Immunol* (2021).
46. Alfen, J.S.*, et al.* Intestinal IFN-gamma-producing Tr1-cells co-express CCR5 and PD-1, and down-regulate IL-10 in the inflamed guts of IBD patients. *J Allergy Clin Immunol* (2018).
47. Kivisakk, P.*, et al.* Natalizumab treatment is associated with peripheral sequestration of proinflammatory T cells. *Neurology* **72**, 1922-1930 (2009).

48. Hrastelj, J.*, et al.* CSF-resident CD4(+) T-cells display a distinct gene expression profile with relevance to immune surveillance and multiple sclerosis. *Brain Commun* **3**, fcab155 (2021).
49. Codarri, L.*, et al.* RORgammat drives production of the cytokine GM-CSF in helper T cells, which is essential for the effector phase of autoimmune neuroinflammation. *Nature immunology* **12**, 560-567 (2011).
50. Paroni, M.*, et al.* Recognition of viral and self-antigens by TH1 and TH1/TH17 central memory cells in patients with multiple sclerosis reveals distinct roles in immune surveillance and relapses. *J Allergy Clin Immunol* (2017).
51. Gordon, J. CD40 and its ligand: central players in B lymphocyte survival, growth, and differentiation. *Blood Rev* **9**, 53-56 (1995).
52. Tschochner, M.*, et al.* Identifying Patient-Specific Epstein-Barr Nuclear Antigen-1 Genetic Variation and Potential Autoreactive Targets Relevant to Multiple Sclerosis Pathogenesis. *PLoS One* **11**, e0147567 (2016).
53. Geginat, J.*, et al.* The light and the dark sides of Interleukin-10 in immune-mediated diseases and cancer. *Cytokine & growth factor reviews* (2016).
54. Yogev, N.*, et al.* CD4(+) T-cell-derived IL-10 promotes CNS inflammation in mice by sustaining effector T cell survival. *Cell Rep* **38**, 110565 (2022).
55. Dardalhon, V., Korn, T., Kuchroo, V.K. & Anderson, A.C. Role of Th1 and Th17 cells in organ-specific autoimmunity. *J Autoimmun* **31**, 252-256 (2008).
56. Haile, Y.*, et al.* Granzyme B-inhibitor serpina3n induces neuroprotection in vitro and in vivo. *J Neuroinflammation* **12**, 157 (2015).
57. Bjornevik, K.*, et al.* Longitudinal analysis reveals high prevalence of Epstein-Barr virus associated with multiple sclerosis. *Science* **375**, 296-301 (2022).
58. Lunemann, J.D.*, et al.* EBNA1-specific T cells from patients with multiple sclerosis cross react with myelin antigens and co-produce IFN-gamma and IL-2. *The Journal of experimental medicine* **205**, 1763-1773 (2008).
59. Wucherpfennig, K.W. & Strominger, J.L. Molecular mimicry in T cell-mediated autoimmunity: viral peptides activate human T cell clones specific for myelin basic protein. *Cell* **80**, 695-705 (1995).
60. Facciotti, F.*, et al.* IL-10-producing forkhead box protein 3-negative regulatory T cells inhibit B-cell responses and are involved in systemic lupus erythematosus. *J Allergy Clin Immunol* **137**, 318-321 e315 (2016).
61. Lanzavecchia, A. Antigen-specific interaction between T and B cells. *Nature* **314**, 537-539 (1985).
62. Jochum, S., Moosmann, A., Lang, S., Hammerschmidt, W. & Zeidler, R. The EBV immunoevasins vIL-10 and BNLF2a protect newly infected B cells from immune recognition and elimination. *PLoS Pathog* **8**, e1002704 (2012).
63. Saraste, M., Penttila, T.L. & Airas, L. Natalizumab treatment leads to an increase in circulating CXCR3-expressing B cells. *Neurol Neuroimmunol Neuroinflamm* **3**, e292 (2016).
64. Lossius, A.*, et al.* High-throughput sequencing of TCR repertoires in multiple sclerosis reveals intrathecal enrichment of EBV-reactive CD8+ T cells. *Eur J Immunol* **44**, 3439-3452 (2014).
65. Magliozzi, R.*, et al.* B-cell enrichment and Epstein-Barr virus infection in inflammatory cortical lesions in secondary progressive multiple sclerosis. *J Neuropathol Exp Neurol* **72**, 29-41 (2013).

66. Serafini, B.*, et al.* Dysregulated Epstein-Barr virus infection in the multiple sclerosis brain. *J Exp Med* **204**, 2899-2912 (2007).
67. Serafini, B.*, et al.* Epstein-Barr virus latent infection and BAFF expression in B cells in the multiple sclerosis brain: implications for viral persistence and intrathecal B-cell activation. *J Neuropathol Exp Neurol* **69**, 677-693 (2010).
68. Angelini, D.F.*, et al.* Increased CD8+ T cell response to Epstein-Barr virus lytic antigens in the active phase of multiple sclerosis. *PLoS Pathog* **9**, e1003220 (2013).
69. Serafini, B., Rosicarelli, B., Veroni, C., Mazzola, G.A. & Aloisi, F. Epstein-Barr Virus-Specific CD8 T Cells Selectively Infiltrate the Brain in Multiple Sclerosis and Interact Locally with Virus-Infected Cells: Clue for a Virus-Driven Immunopathological Mechanism. *J Virol* **93**(2019).
70. Balashov, K.E., Rottman, J.B., Weiner, H.L. & Hancock, W.W. CCR5(+) and CXCR3(+) T cells are increased in multiple sclerosis and their ligands MIP-1alpha and IP-10 are expressed in demyelinating brain lesions. *Proc. Natl. Acad. Sci. U. S. A.* **96**, 6873-6878 (1999).
71. Schneider-Hohendorf, T.*, et al.* Broader Epstein-Barr virus-specific T cell receptor repertoire in patients with multiple sclerosis. *J Exp Med* **219**(2022).
72. Zdimerova, H.*, et al.* Attenuated immune control of Epstein-Barr virus in humanized mice is associated with the multiple sclerosis risk factor HLA-DR15. *Eur J Immunol* **51**, 64-75 (2021).
73. Magliozzi, R.*, et al.* Meningeal B-cell follicles in secondary progressive multiple sclerosis associate with early onset of disease and severe cortical pathology. *Brain* **130**, 1089-1104 (2007).
74. Pender, M.P., Csurhes, P.A., Burrows, J.M. & Burrows, S.R. Defective T-cell control of Epstein-Barr virus infection in multiple sclerosis. *Clin Transl Immunology* **6**, e126 (2017).

Figure 1

A

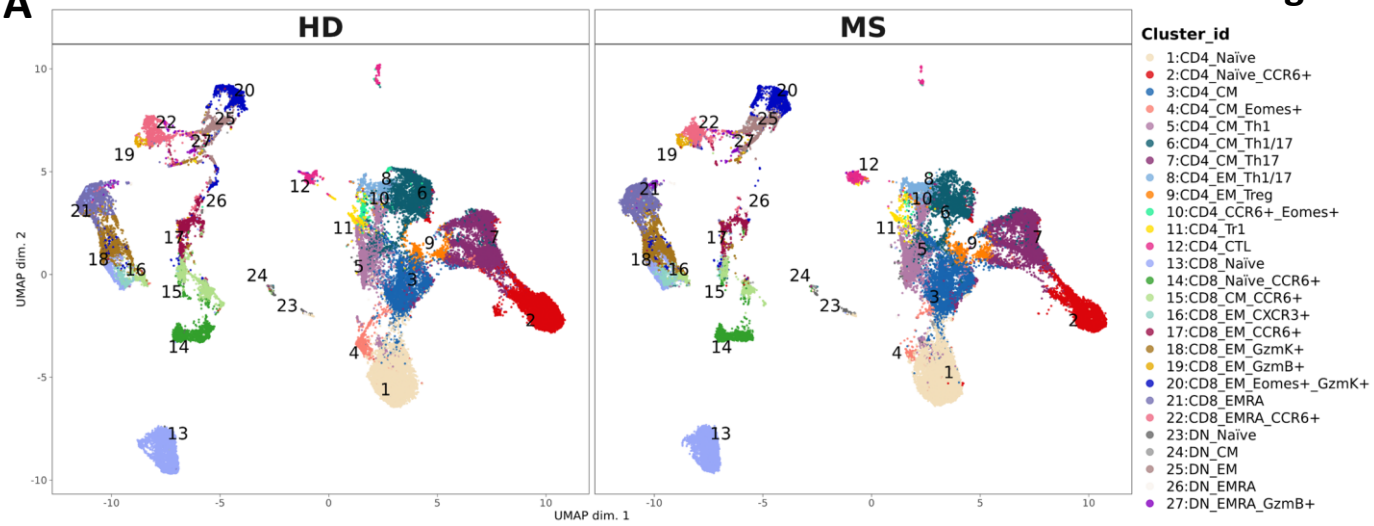

B

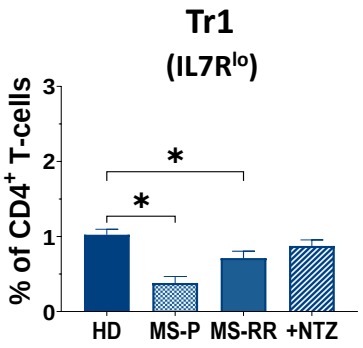

C

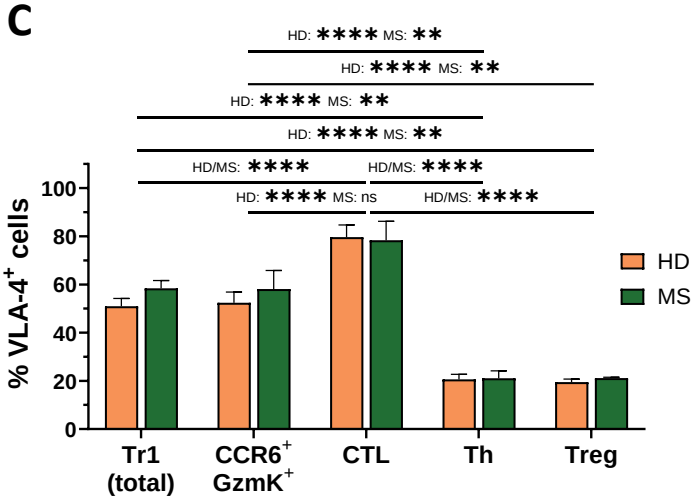

D

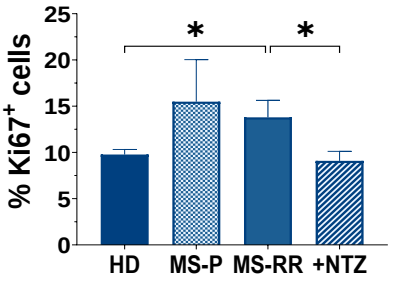

Figure 2

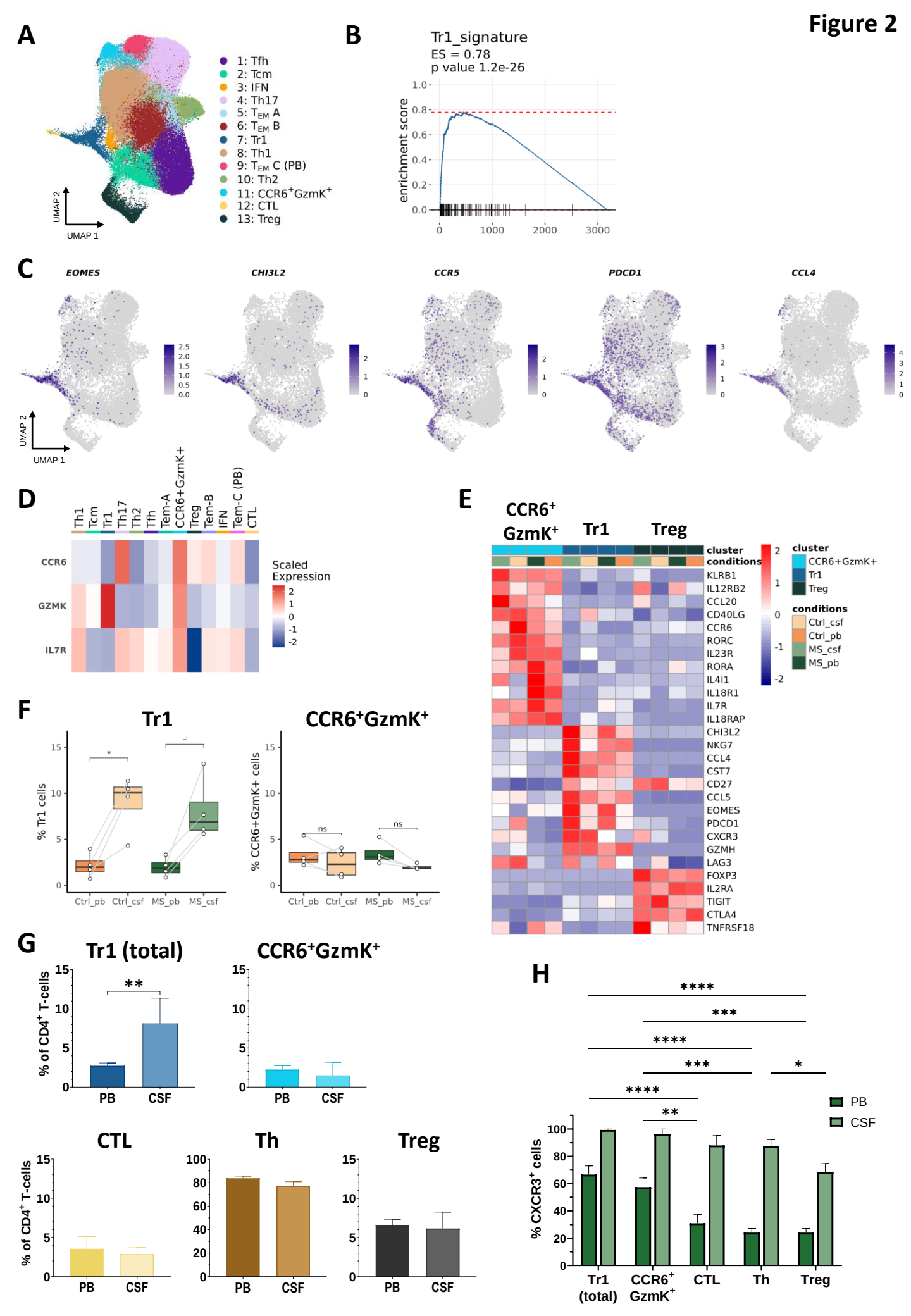
A
1: Tfh
2: Tcm
3: IFN
4: Th17
5: T_EM A
6: T_EM B
7: Tr1
8: Th1
9: T_EM C (PB)
10: Th2
11: CCR6+GzmK+
12: CTL
13: Treg
UMAP 2
UMAP 1
B
Tr1_signature
ES = 0.78
p value 1.2e-26
enrichment score
C
EOMES
CHI3L2
CCR5
PDCD1
CCL4
D
Th1
Tcm
Tr1
Th17
Th2
Tfh
Tem-A
CCR6+GzmK+
Treg
Tem-B
IFN
Tem-C (PB)
CTL
CCR6
GZMK
IL7R
Scaled Expression
E
CCR6+ GzmK+
Tr1
Treg
cluster
conditions
KLRB1
IL12RB2
CCL20
CD40LG
CCR6
RORC
IL23R
RORA
IL4I1
IL18R1
IL7R
IL18RAP
CHI3L2
NKG7
CCL4
CST7
CD27
CCL5
EOMES
PDCD1
CXCR3
GZMH
LAG3
FOXP3
IL2RA
TIGIT
CTLA4
TNFRSF18
CCR6+GzmK+
Tr1
Treg
Ctrl_csf
Ctrl_pb
MS_csf
MS_pb
F
Tr1
CCR6+GzmK+
% Tr1 cells
% CCR6+GzmK+ cells
Ctrl_pb
Ctrl_csf
MS_pb
MS_csf
ns
G
Tr1 (total)
CCR6+GzmK+
% of CD4+ T-cells
PB
CSF
CTL
Th
Treg
H
% CXCR3+ cells
PB
CSF
Tr1 (total)
CCR6+ GzmK+
CTL
Th
Treg

Figure 3

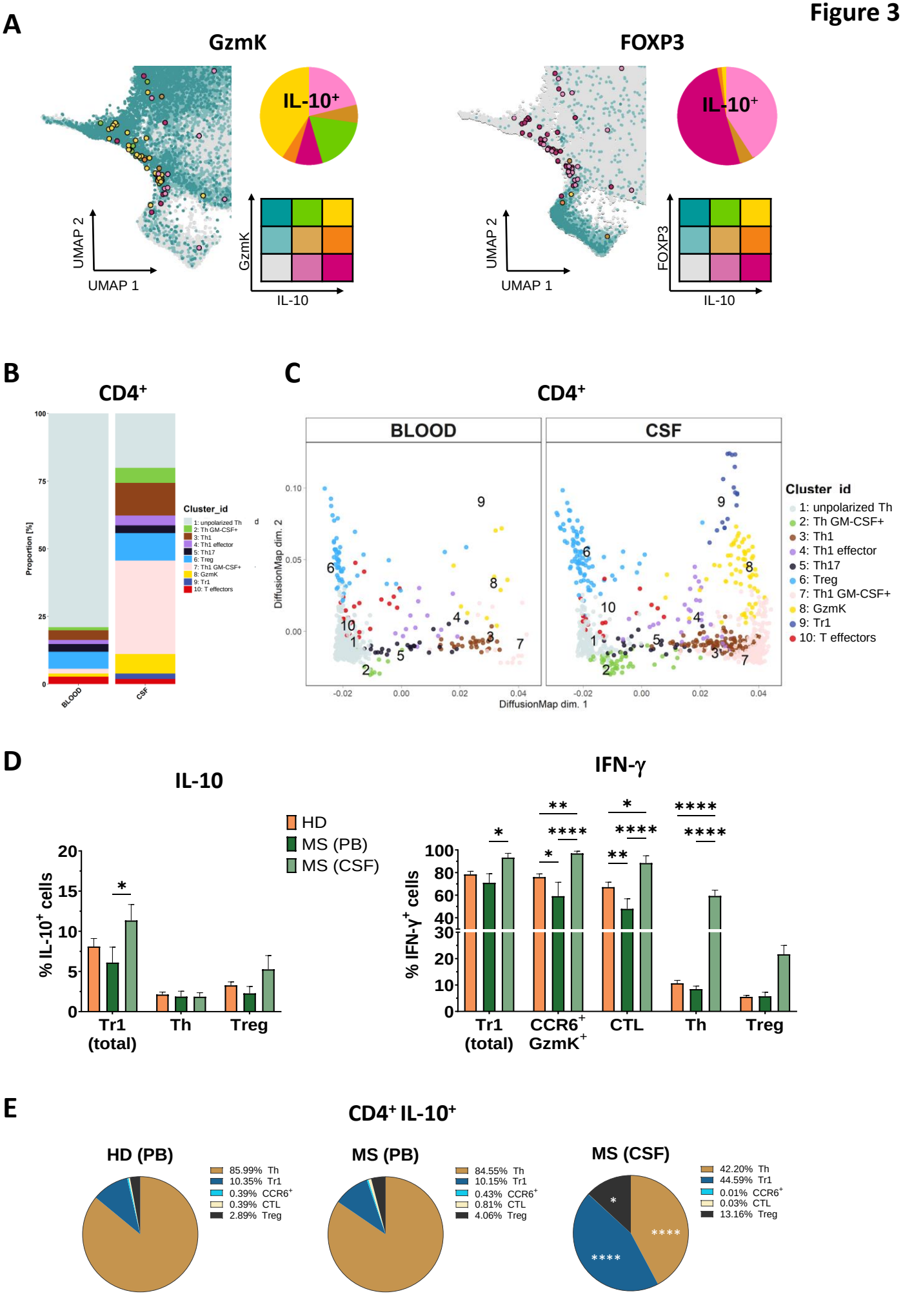
A
GzmK
FOXP3
IL-10+
UMAP 2
UMAP 1
GzmK
FOXP3
IL-10
B
CD4+
Proportion [%]
BLOOD
CSF
Cluster_id
1: unpolarized Th
2: Th GM-CSF+
3: Th1
4: Th1 effector
5: Th17
6: Treg
7: Th1 GM-CSF+
8: GzmK
9: Tr1
10: T effectors
C
CD4+
BLOOD
CSF
DiffusionMap dim. 2
DiffusionMap dim. 1
Cluster_id
1: unpolarized Th
2: Th GM-CSF+
3: Th1
4: Th1 effector
5: Th17
6: Treg
7: Th1 GM-CSF+
8: GzmK
9: Tr1
10: T effectors
D
IL-10
IFN-γ
HD
MS (PB)
MS (CSF)
% IL-10+ cells
% IFN-γ+ cells
Tr1 (total)
Th
Treg
CCR6+ GzmK+
CTL
E
CD4+ IL-10+
HD (PB)
85.99% Th
10.35% Tr1
0.39% CCR6+
0.39% CTL
2.89% Treg
MS (PB)
84.55% Th
10.15% Tr1
0.43% CCR6+
0.81% CTL
4.06% Treg
MS (CSF)
42.20% Th
44.59% Tr1
0.01% CCR6+
0.03% CTL
13.16% Treg

Figure 4

A

MOG/ MBP

EBV

JCV

CD4

% IFN-γ+CD69+ of CD4+

Th ***

Tr1 ****/*

Tr1 **/ns

Th **

Th *

***

Treg

Th

CTL

CCR6+

Tr1 IL-7R+

Tr1 IL-7Rlo

HD

MS

+NTZ

B

Treg

% CD69+ of CD4+

*

4-1BB

***

4-1BB

**

4-1BB

*

4-1BB

4-1BB

4-1BB IFN-γ

IFN-γ

♦Paired t-test vs Ctr-

C

Th1 lines (CSF, MS)

% IFN-γ+ cells

CTR -

EBV

MOG/ MBP

Eomes+

Eomes-

D

EBNA1

BZLF1

% IFN-γ+CD69+ of CD4+

Th **

Tr1IL-7Rlo

E

IL-10

Tr1 (total)

Treg

% IL-10+ of CD4+

EBV

EBNA1

MOG-MBP

F

SLE

EBV (Pool)

EBNA1

% IFN-γ+ of CD4+

+CNS

Figure 5

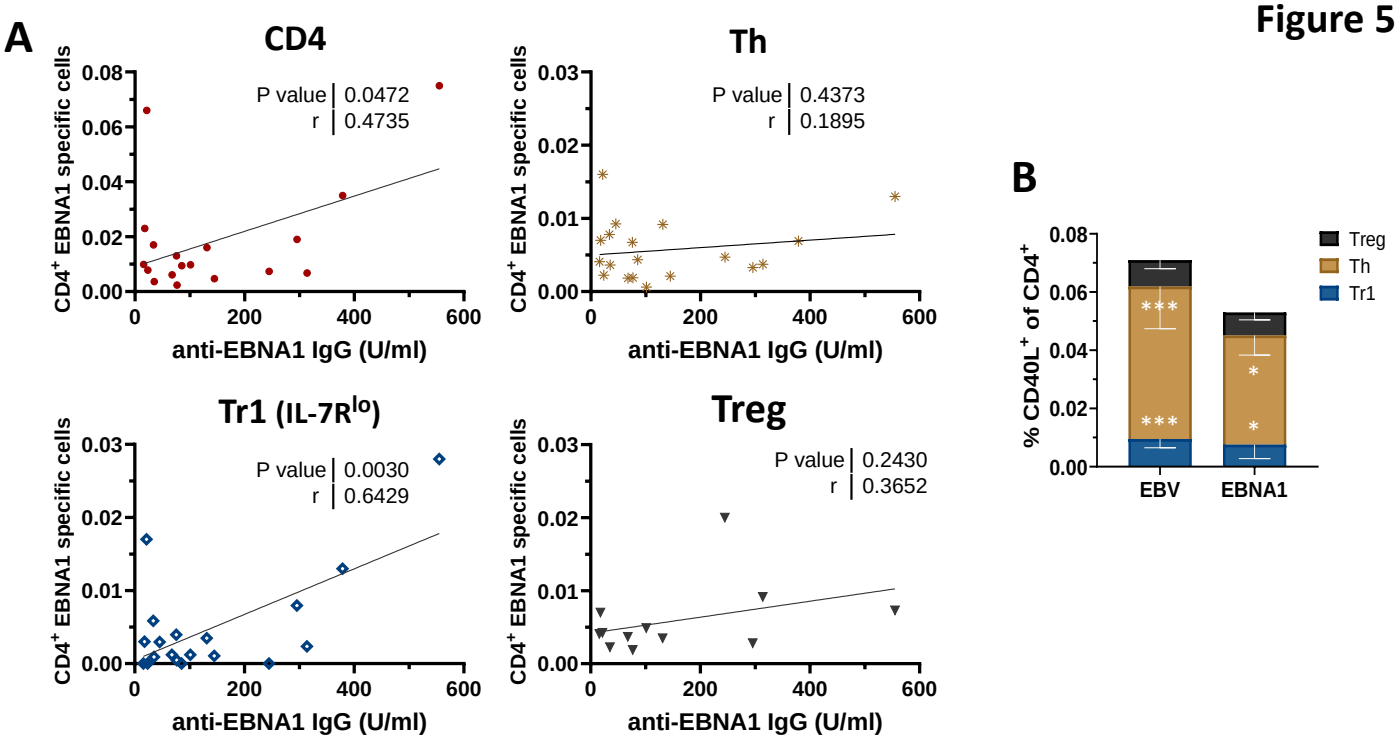
A
CD4
P value | 0.0472
r | 0.4735
Th
P value | 0.4373
r | 0.1895
Tr1 (IL-7R^{lo})
P value | 0.0030
r | 0.6429
Treg
P value | 0.2430
r | 0.3652
CD4$^+$ EBNA1 specific cells
anti-EBNA1 IgG (U/ml)
B
% CD40L$^+$ of CD4$^+$
Treg
Th
Tr1
EBV
EBNA1

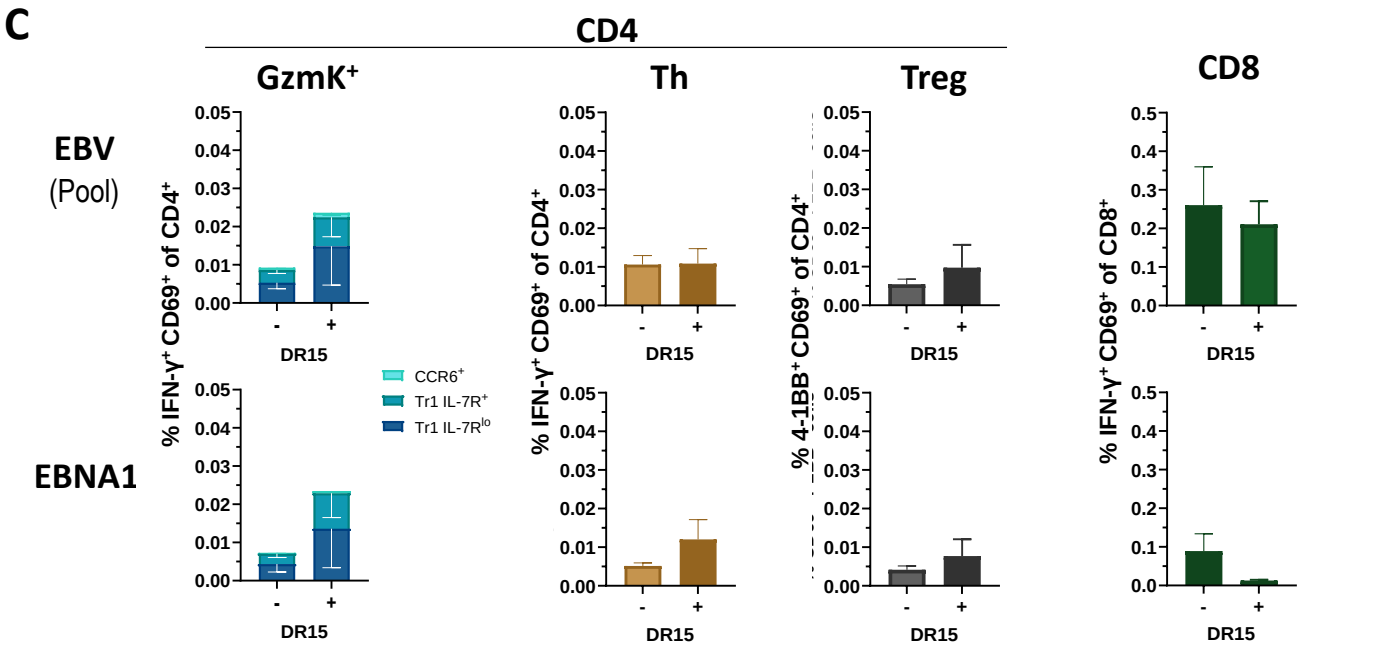
C
CD4
GzmK$^+$
Th
Treg
CD8
EBV
(Pool)
EBNA1
% IFN-γ$^+$ CD69$^+$ of CD4$^+$
% IFN-γ$^+$ CD69$^+$ of CD8$^+$
% 4-1BB$^+$ CD69$^+$ of CD4$^+$
DR15
CCR6$^+$
Tr1 IL-7R$^+$
Tr1 IL-7R^{lo}

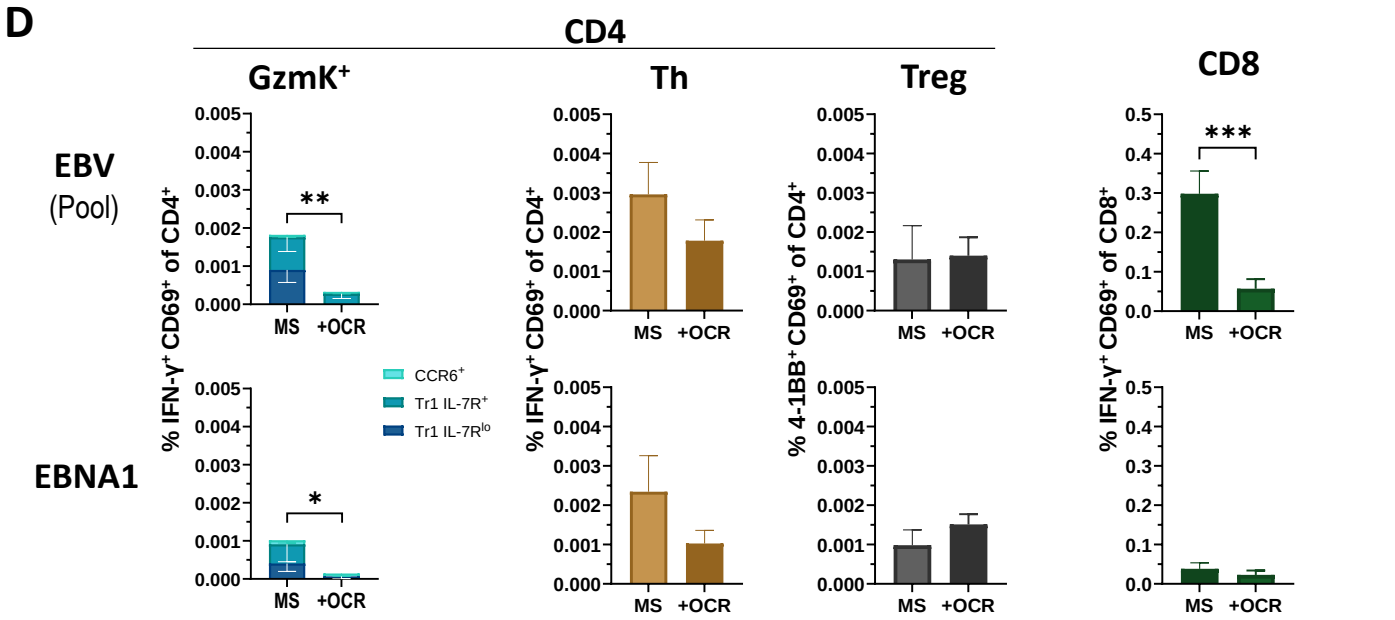
D
CD4
GzmK$^+$
Th
Treg
CD8
EBV
(Pool)
EBNA1
% IFN-γ$^+$ CD69$^+$ of CD4$^+$
% IFN-γ$^+$ CD69$^+$ of CD8$^+$
% 4-1BB$^+$ CD69$^+$ of CD4$^+$
MS
+OCR
CCR6$^+$
Tr1 IL-7R$^+$
Tr1 IL-7R^{lo}

Figure 6

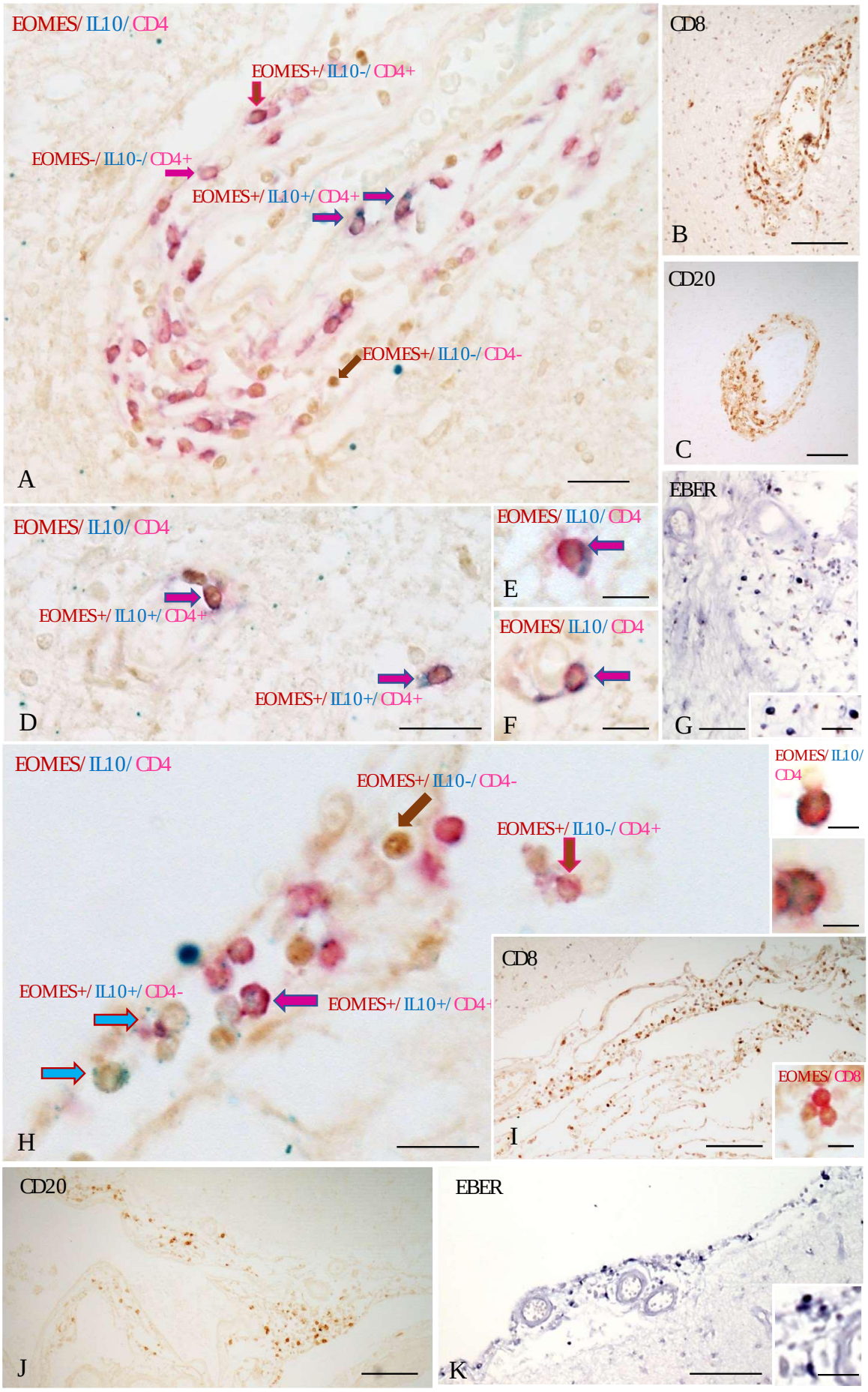
EOMES/ IL10/ CD4
EOMES+/ IL10-/ CD4+
EOMES-/ IL10-/ CD4+
EOMES+/ IL10+/ CD4+
EOMES+/ IL10-/ CD4-
A
CD8
B
CD20
C
EBER
G
EOMES/ IL10/ CD4
EOMES+/ IL10+/ CD4+
EOMES+/ IL10+/ CD4+
D
EOMES/ IL10/ CD4
E
EOMES/ IL10/ CD4
F
EOMES/ IL10/ CD4
EOMES+/ IL10-/ CD4-
EOMES+/ IL10-/ CD4+
EOMES+/ IL10+/ CD4-
EOMES+/ IL10+/ CD4-
H
EOMES/ IL10/ CD4
CD8
EOMES/ CD8
I
CD20
J
EBER
K